

Universidade do Minho
Escola de Ciências

Ana Sofia Pontes Castanheiro

**Bioaccumulation and toxicology of nanomaterials
used by the plastic industry in marine mussels**



Universidade do Minho
Escola de Ciências

Ana Sofia Pontes Castanheiro

**Bioaccumulation and toxicology of nanomaterials
used by the plastic industry in marine mussels**

Master Thesis
Master in Biophysics and Bionanossystems

Work developed under the supervision of
Dr. Begoña Espiña
and
Prof. Dr. Andreia Gomes

January 2020

DIREITOS DE AUTOR E CONDIÇÕES DE UTILIZAÇÃO DO TRABALHO POR TERCEIROS

Este é um trabalho académico que pode ser utilizado por terceiros desde que respeitadas as regras e boas práticas internacionalmente aceites, no que concerne aos direitos de autor e direitos conexos.

Assim, o presente trabalho pode ser utilizado nos termos previstos na licença abaixo indicada.

Caso o utilizador necessite de permissão para poder fazer um uso do trabalho em condições não previstas no licenciamento indicado, deverá contactar o autor, através do RepositóriUM da Universidade do Minho.

Licença concedida aos utilizadores deste trabalho



Atribuição-NãoComercial-SemDerivações

CC BY-NC-ND

<https://creativecommons.org/licenses/by-nc-nd/3.0/pt/>

Acknowledgments

I would like to thank the INL - International Iberian Nanotechnology Laboratory for providing me the required conditions to make possible the execution of this work.

I am grateful to Dr. Begoña Espiña and Dr. Andreia Gomes, my supervisors, for the constant availability to help, clarifying doubts and making suggestions in order to improve this work, their patient guidance and dedication, allowing its accomplishment. My sincere thanks need to be extended to Ivone Pinheiro and Laura Rodriguez for their time and wise advices every time I needed help, following all the steps, although not being my supervisors.

I also must thank to all the Water Quality, past and present, group members, for being there every time, in and out the lab supporting me during the project development.

Finally, but by no means least, I must express my gratitude to my parents and my brother for their huge patience, for investing in my education and in my dreams and all the unfailing support during this year.

This Master thesis is within the scope of the Interreg SUDOE NanoDesk funded project whose goal is to create a set of advanced web-based tools to promote the application of Nanotechnology and safe use of nanomaterials in the plastic industry in the south-west Europe region.

Statement of integrity

I hereby declare having conducted this academic work with integrity. I confirm that didn't use plagiarism or any other form of misuse of information or results falsification along its elaboration.

I further declare that I have fully acknowledged the Code of Ethical Conduct of the University of Minho.

Título: Bioacumulação e toxicologia de nanomateriais utilizados na indústria do plástico, em mexilhões marinhos.

Resumo: A nanotecnologia tem vindo a desenvolver-se exponencialmente nos últimos anos e está a tornar-se a tecnologia mais avançada deste milénio. Apesar dos benefícios, este crescimento cria também a necessidade de compreender os possíveis riscos, forçando a nanotoxicologia a crescer em simultâneo. Os plásticos tornaram-se indispensáveis para um número ilimitado de atividades humanas e o seu destino final parece impossível de controlar. Assim, é imperativo compreender os possíveis efeitos tóxicos associados não só aos plásticos em si, mas também às nanopartículas que podem ser libertados aquando da sua degradação. Nanopartículas que são tipicamente incorporadas na matriz dos polímeros com o objetivo de melhorar as suas propriedades físico-químicas.

Mexilhões marinhos, tal como o *Mytilus galloprovincialis*, são amplamente utilizados como modelo quer para testes ecotoxicológicos como para testes de controlo alimentar. O seu habitat e forma de alimentação fazem deles bons biomonitores para estudos de bioacumulação de contaminantes em água. Este estudo reforça resultados já reportados por relatórios anteriores que revelam a bioacumulação de nanomateriais utilizados na indústria, em organismo aquáticos, mostrando que as nanopartículas de Ag, TiO₂ e ZnO são incorporadas de diferentes formas nos mexilhões *Mytilus galloprovincialis* ao fim de 28 dias de exposição.

Palavras-chave: Plásticos, Nanomateriais, Bioacumulação, *Mytilus galloprovincialis*

Title: Bioaccumulation and toxicology of nanomaterials used by the plastic industry in marine mussels.

Abstract: Nanotechnology has been developing exponentially in recent years and is becoming the most advanced technology in the third millennium. Despite the benefits, this growth also creates the need to understand its possible risks, forcing nanotoxicology to expand simultaneously.

Plastics have become indispensable in an unlimited range of human activities and their final fate seems impossible to control. Therefore, it is imperative to understand the possible toxicity effects related not only to these materials, but also to the released nanoparticles resulting from their degradation. Such nanoparticles are typically incorporated into the polymers matrix to improve the plastic's physicochemical properties.

Marine mussels, such as *Mytilus galloprovincialis*, are a widely used model for both ecotoxicological and food safety tests. Their habitat and feeding form make them valuable bio-monitors for water contaminants bioaccumulation studies.

This study reinforces the notions gathered from previously published reports that reveal bioaccumulation of engineered nanomaterials in aquatic organisms, showing that Ag, TiO₂ and ZnO nanoparticles are incorporated in different ways in mussels *Mytilus galloprovincialis* after 28 days of exposure.

Keywords: Plastic, Engineered nanomaterials, Bioaccumulation, *Mytilus galloprovincialis*

Index

I.	Introduction	12
1.	Nanotechnology in the plastic industry.....	12
1.1	Silver nanoparticles	15
1.2	Titanium dioxide nanoparticles.....	15
1.3	Zinc Oxide	16
2.	Marine Mussel – <i>Mytilus galloprovincialis</i> - as a model for bioaccumulation	18
II.	Materials and Methods.....	21
1.	Chemicals and reagents.....	21
2.	Engineered nanomaterials dispersion	21
3.	Dynamic Light Scattering.....	22
4.	Inductively Coupled Plasma - Optical Emission Spectrometry	22
5.	Sample preparation: mussels' tissue digestion and ENMs dissolution.....	25
6.	Transmission Electron Microscopy.....	25
7.	Scanning Electron Microscopy.....	26
8.	Mussels maintenance and exposure	27
9.	Statistical analysis.....	28
III.	Results	29
1.	Ecotoxicity.....	29
I.	Survival.....	29
II.	Mussels morphometric parameters.....	30
2.	Physicochemical seawater parameters	31
3.	Optimization of ICP-OES sample preparation: mussels' tissue digestion and ENMs dissolution	31
4.	Silver nanoparticles stability and bioaccumulation.....	33
5.	Titanium dioxide.....	38
6.	Zinc Oxide.....	41
IV.	Conclusions	44
V.	Future perspectives.....	45
VI.	References.....	46

Abbreviations

EU	European Union
REACH	Registration, Evaluation, Authorization and Restriction of Chemicals
CLP	Classification, Labelling and Packaging
ENMs	Engineered nanomaterials
Ag NPs	Silver nanoparticles
TiO ₂ NPs	Titanium dioxide nanoparticles
LC ₅₀	Lethal concentration
LD ₅₀	Lethal dose
ZnO NPs	Zinc oxide nanoparticles
Tris	Trizma® base
DLS	Dynamic light scattering
ICP-OES	Inductively coupled plasma-optical emission spectrometry
LOD	Limit of detection
LOQ	Limit of quantification
S _b	ICP-OES signal of blanks samples
SD _b	Standard deviation of blank's intensities
TEM	Transmission electron microscopy
EDX	Energy-dispersive X-ray
SEM	Scanning electron microscopy
PEC	Predicted environmental concentration

Table index

Table 1: Sonication conditions for ENMs dispersion in solution to be applied in mussel bioaccumulation study.....	22
Table 2: ICP-OES conditions	24
Table 3: Recovery rate values from ICP-OES samples digestion protocols, with and without enzymatic digestion step with Neutrase®.....	32

i. Figure index

Figure 1: Sketch representing plastics for different applications. Adapted from [8].	13
Figure 2: Albatross chicks threatened by plastic entanglement (left) and ingestion (right), on National Marine Sanctuary, on Midway Atoll (United States). Adapted from [16].	14
Figure 3: Scheme resuming which properties engineered nanomaterials can improve in different sectors. Adapted from [45].	17
Figure 4: Photo of <i>Mytilus galloprovincialis</i> specimens in an artificial saltwater tank.	18
Figure 5: Photo in a sketch representing <i>Mytilus galloprovincialis</i> morphology. Adapted from [48].	19
Figure 6: ICP-OES calibration curve for all the ENMs. 11-point external calibration curve from 0 to 2 mg/L (ppm) for Ag, TiO ₂ and Zn.	24
Figure 7: Evaluation of mortality rate for different ENMs concentrations in saltwater after 24 hours, 7, 14, 21 and 28 days of exposure (T0, T1, T2, T3 and T4, respectively) of exposure. The statistical data was obtained by chi-square test.	29
Figure 8: Photo of a closed <i>Mytilus galloprovincialis</i> mussel with a sketch representing morphometric measurements, length of the mussel's shell (M1) and width of the shell (M2).	30
Figure 9: Silver (Ag) quantification by ICP-OES , in soft tissue mussel samples collected after 24 hours, 7, 14, 21 and 28 days of exposure (T0, T1, T2, T3 and T4, respectively) of exposure, from a random replica of each condition (F (8, 30) = 2.77, P= 0.02).	33
Figure 10: TEM picture of hepatopancreas tissue extracted from a mussel exposed to 0 mg/L (A) and 1 mg/L (B) of silver nanoparticles for 28 days (50 000x magnification; 200 kV voltage). Within the red circle is possible to observe a nanoparticle aggregated.	35
Figure 11: TEM picture of hepatopancreas tissue extracted from a mussel exposed to 1 mg/L of silver nanoparticles for 28 days (300 000x magnification; 200 kV voltage). Within the square is possible to observe a nanoparticle, supposedly silver, and its crystalline planes.	35
Figure 12: TEM picture of grid spiked with a silver nanoparticles solution (1 000 000x magnification; 200 kV voltage). Is possible to observe a silver nanoparticle aggregate and the nanoparticles crystalline planes.	36
Figure 13: SEM picture of the outer shell surface belonging to a mussel exposed to 1 mg/L of silver nanoparticles for 28 days. In the picture it is possible to observe some nanoparticles in the shell surface.	37
Figure 14: SEM picture of the outer shell surface with a 100 mg/L silver nanoparticles solution on the surface. In the picture is possible to observe small and shining nanoparticles dispersed throughout the shell surface.	37
Figure 15: Titanium dioxide (TiO₂) quantification by ICP-OES , in soft tissue mussel samples collected after 24 hours, 7, 14, 21 and 28 days of exposure (T0, T1, T2, T3 and T4, respectively) of exposure, from a random replica of each condition (F (8, 30) = 4193, P< 0.0001).	38
Figure 16: TEM picture of hepatopancreas tissues extracted from a mussel exposed to 1 mg/L (A) and 0 mg/L (B) of titanium dioxide for 28 days (A: 30 000x magnification and B: 15 000x magnification; both with 200 kV voltage).	39
Figure 17: TEM picture of grid spiked with a titanium dioxide nanoparticles solution. (100 000x and 400 000x magnification with 200 kV voltage).	40
Figure 18: SEM pictures of the outer shell surface belonging to a mussel exposed to 1 mg/L of titanium dioxide nanoparticles for 28 days. In picture A is possible to observe micro sized aggregates disperse	

trough the surface, in B is possible to observe one presented in A but with more detail (high magnification)..... 40

Figure 19: EDX spectrum showing chemical composition of an aggregate present on a mussel's shell surface. Within the black circles it is possible to confirm the presence of significant amount of titanium and oxygen elements. 41

Figure 20: Zinc oxide (ZnO) quantification by ICP-OES, in soft tissue mussel samples collected after 24 hours, 7, 14, 21 and 28 days of exposure (T0, T1, T2, T3 and T4, respectively) of exposure, from a random replica of each condition (F (12, 40) = 10.71, P< 0.0001)..... 42

Figure 21: SEM picture of the outer shell surface belonging to a mussel exposed to 1 mg/L of zinc oxide nanoparticles for 28 days. In the picture it is possible to observe micro sized aggregates adsorbed to the surface. 43

Figure 22: SEM picture of the outer shell surface with a 100 mg/L silver nanoparticles solution on the surface. In the picture is possible to observe micro sized aggregates dispersed to the surface..... 43

I. Introduction

1. Nanotechnology in the plastic industry

Nanotechnology has been developing abruptly in recent years and is becoming the most advanced technology in the third millennium. This growth offers significant benefits to mankind, but also carries new hazards and risks which forces nanotoxicology to expand simultaneously [1].

The fundamental reason for this concern regarding nanoparticles and nanomaterials is that, when materials of such small dimensions are present, these may behave chemically, physically and toxicologically differently from their bulk material, and these demeanors are hardly predictable. In the worst case, it must be considered that any material might be toxicologically effective, or more active, when presented to the body in nanoform, which implies a more immediate toxicological exam [1,2].

In the plastic industry specifically, the application of nanotechnology is mainly associated with the incorporation of nanosized additives (materials with dimensions between 1 and 100 nm), commonly called nanofillers, into the polymer matrix in order to improve mechanical, electrical and thermal properties of these new plastic materials, such as oxygen barrier properties or heat resistance [3–5].

Since the mid-20th century, plastics have been widely used in an unlimited range of human activities and plastic items have become indispensable [6,7]. Plastics are not just one material, but instead, are a whole family of hundreds of different materials and their unique properties make them meet the needs of an ample range of different application sectors such as packaging, building and construction, automotive and aeronautics, electrical and electronic equipment, leisure and sports clothes or medical and health products (Figure 1) [8].



Figure 1: Sketch representing plastics for different applications. Adapted from [8].

The global production of plastics is increasing exponentially since the 1950s and is projected to reach around 1800 million tons in 2050 [9,10]. Many countries still have inefficient waste management and water treatment systems allowing leakage to the environment and, consequently, the amount that reaches the oceans on a global scale is largely unknown [9, 11, 12]. Besides that, plastic is designed to be durable, persisting in the environment for long periods of time [12].

In 2016, a study along the eastern coast of Brazil highlighted that edible fish were ingesting microplastics (22% of the marine fish studied had plastic pellets in their stomachs) [13]. In the same year, after seeding thousands of clams and oysters across coast and analyzing them after three months, a shellfish biologist claimed that if we eat clams and oysters, we are eating plastic [14]. More recently, microplastic was found in polar regions, including Arctic beaches, sea ice and deep seafloor, reinforcing the idea of aerial transport, since there are not many ways to explain how microplastics travel such distances [12]. Plastic pollution is global, but ocean's related plastic pollution is particularly impactful and images of marine animals surrounded by and ingesting plastic have become common (Figure 2), so plastic turned into a focus in the media worldwide partly through designing simple lifestyle changes, such as reusable water bottles, trying to provide a "quick fix" technological solutions to this problem, such as large scale clean-up operations and new "biodegradable" plastic substitutes [15].



Figure 2: Albatross chicks threatened by plastic entanglement (left) and ingestion (right), on National Marine Sanctuary, on Midway Atoll (United States). Adapted from [16].

Plastic products have a short useful life and, when discarded indiscriminately, they are degraded into smaller pieces across different physical and chemical processes, that can take them to become micro/nanoplastics and releasing the nanoparticles that were incorporated into them. Some of these nanomaterials could probably persist for centuries in the environment and, despite their abundance, possible toxicity mechanisms are largely unknown [11].

Current legislations do not require a complete knowledge of the consequences of nanoparticles used in consumer goods, except for areas like food, exposure at work or pharmaceutical applications and, since this practice is increasing rapidly, new laws and consequently more studies are needed to ensure that nanoparticles are safe [1,17]. Currently, in the European Union (EU), there are two main regulations that control chemicals use: The Registration, Evaluation, Authorization and Restriction of Chemicals (REACH) and the Classification, Labelling and Packaging (CLP) regulation. REACH was developed in order to protect human health and environment from the chemicals risks while promotes alternative methods, enhancing the competitiveness of the EU chemicals industry. CLP complements REACH, ensures the secure and free movement of substances, mixtures and articles, forcing their classification and labelling [18]. Since neither REACH nor CLP provided any explicit requirements for nanomaterials, a new recommendation on the definition of a nanomaterial and REACH actualization was released by the European Commission, in December 2018 [18, 19].

More than 1200 scientific papers reporting effects of engineered nanomaterials (ENMs) were compiled by the Danish Environmental Protection Agency [20]. Almost a third of these revealed data on acute and chronic effects on relevant organisms, including studies in algae, fish and freshwater invertebrates.

Nevertheless, there is a distinct lack of studies from environments other than freshwater and a low diversity of tested organisms as well as trophic levels [20].

Given all this, and considering current availability on the market, potential applications in polymeric matrices, production volumes, cost and toxicological profiles, we will briefly describe the four ENMs chosen to be studied in this work.

1.1 Silver nanoparticles

Silver nanoparticles (AgNPs)-based, and AgNPs-containing consumer products have increased in the last years due to their known applications in different areas, and intrinsic therapeutic properties [21–23]. The latter lead to increasing release of AgNPs into the aquatic environment, which also requires the identification of possible risks to the environment and health [24–26]. When included in the materials, such as plastics, AgNPs, can improve optical, electrical and thermal conductivity and provide antimicrobial properties [23]. In previous studies, AgNPs did not present cytotoxicity when functionalized to attach to a specific target [21], in contrast, for the non-functionalized nanoparticles, the toxicity was shown to depend on many factors such as size, concentration, dispersion and exposure mode [22,23]. There are some reports that describe that silver nanoparticles can penetrate in cellular compartments and induce the production of reactive oxygen species leading to cytotoxicity, but these depends on cell type [21,22]. A previous study based on zebrafish embryos toxicity test of silver nanoparticles revealed increased mortality rates, decreased hatchability rate and axial deformity, highlighting the importance of size in nanoparticles possible toxic effects [27]. The major aspects that can affect silver nanoparticles toxicity should alert to the need of more bioaccumulation studies before marketing these AgNPs-based materials [27].

1.2 Titanium dioxide nanoparticles

Titanium dioxide nanoparticles (TiO₂ NPs) are the most produced industrial metal nanoparticles worldwide, and the number of products containing it is increasing. Such an enormous amount availability will inevitably end up in aquatic ecosystems [28,29]. Their unique physical and chemical properties allow for a wide range of applications, which highlights the importance of knowing the possible impacts of TiO₂ NPs in global environmental and public health [28,29]. Due to their high chemical stability, anticorrosive

and photocatalytic properties, TiO₂ NPs are commonly used in paints, coatings, plastics, papers, inks, medicines, pharmaceuticals, cosmetics, toothpaste and food products and packing [30]. TiO₂ NPs can be used in sunscreens, articulating prosthetic implants or even as semiconductor photocatalysis in water treatment [31] and in nanocrystalline solar cells as photoactive material [32].

The major routes of TiO₂ NPs human exposure are inhalation and dermal exposure, during both manufacturing and use. Oral exposure may occur during the use of toothpaste, food colorants and nutritional supplements, or through food contact with the packaging [30].

Despite TiO₂ fine particles have been considered as a low toxicity material, they possess different physicochemical properties which would be expected to alter toxicological properties [30]. TiO₂ nanoparticles acute ecotoxicity tests results are quite diverse, for the same model, *Daphnia magna*, there are reported diverse lethal concentration (LC₅₀) and lethal dose (LD₅₀) values, variations that might be accounted by differences in particle size, stock preparation and test design, for example. Chronic toxicity tests show an effect on reducing offspring survival along with reduction of growth and reproduction in *D. magna* and no adverse effects on *Physa acuta* freshwater snail [33]. In the *Mytilus galloprovincialis*, the effects of TiO₂ NPs have been thoroughly explored revealing, essentially, effects on immune parameters, that result in induced immunomodulation [34–38].

In last year's powders containing 1% or more of TiO₂ NPs, were considered carcinogenic in solution by European Union after the publication of several studies that reveal the appearance of pulmonary tumors after TiO₂ inhalation [39]. Hereupon, there are an unlimited number of animal or cell culture toxicological studies reported, but due to the lack of homogeneity between them, available results are inconclusive, and it is necessary to review, and extrapolate to human exposures. To allow better comparison between data, all future studies on these nanoparticles should characterize their physicochemical properties, such as size distribution, crystalline structure, surface area, coating, as delivered to biological system [30].

1.3 Zinc Oxide

Zinc oxide nanoparticles (ZnO NPs) are one of the most utilized nanomaterials in diverse industrial fields and their production has increased significantly over the past years [40]. Such as in other materials, when the particle size decreases, physic-chemical characteristics of ZnO NPs change providing favorable features for commercial application fields [41]. Despite zinc oxide is normally considered to have low toxicity, the effects of these nanoparticles depend on different factors like size and route of exposure, and

smaller particles have been shown to be the most toxic [40–42]. Studies revealed toxic effects on, mussel *Mytilus galloprovincialis*, earthworm *Eisenia fetida*, *Bacillus subtilis*, *Escherichia coli*, and *Pseudomonas flurencens*, for example, which cause, oxidative stress and DNA damage, mortality and growth inhibition, respectively [41–43].

The quick and continuous growth of engineered nanoparticles use in industrial and household applications (Figure 3) will lead to the increased release of these materials into the environment, and this requires an imperative understanding of their mobility, reactivity, ecotoxicity and persistency [44].

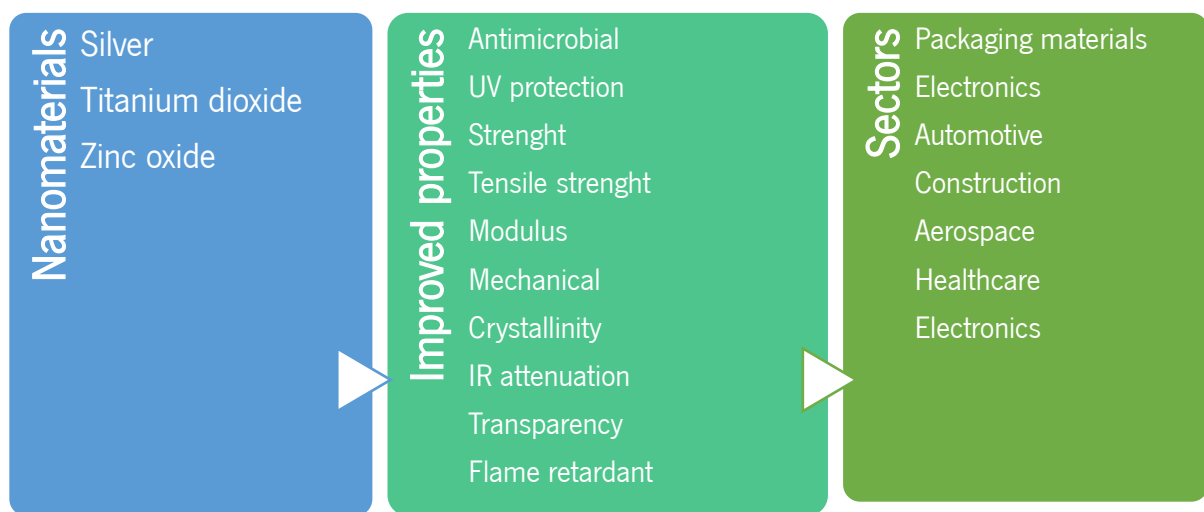


Figure 3: Scheme resuming which properties engineered nanomaterials can improve in different sectors.

Adapted from [45].

2. Marine Mussel – *Mytilus galloprovincialis* - as a model for bioaccumulation

Marine mussels (Figure 4), such as *Mytilus galloprovincialis* (Lamarck, 1819), are filter feeder animals, widely distributed throughout the cooler waters of both northern and southern hemispheres, sedentary and tolerant to different environmental conditions [43,46,47]. Having the rocks through the water column as principal habitat, this species is mainly exposed to dissolved particles, rather than sediments, making them great bio-monitors of coastal water quality [46].



Figure 4: Photo of *Mytilus galloprovincialis* specimens in an artificial saltwater tank.

Mussel's morphology includes shell, mantle, foot, gill, digestive gland, gonad, heart, kidney and nervous tissue (Figure 5). Through the addition of material from the mantle and, calcium and carbonate obtained from diet, the shell grows in circumference and in thickness. The mantle is completely enclosed in the shell, and is constituted of connective tissue with hemolymph vessels, nerves and muscles. The cilia on the mantle's inner part is responsible to directing particles onto the gills, and deflecting heavier material through in, and outcoming water. That, and the slow metabolism plays an important role in the bioaccumulation of organic and non-organic sediments/contaminants in mussel's tissues [43,46–49]. In this work, the sampling tissues for electron microscopy are the digestive gland (hepatopancreas) and mantle, and the shell.

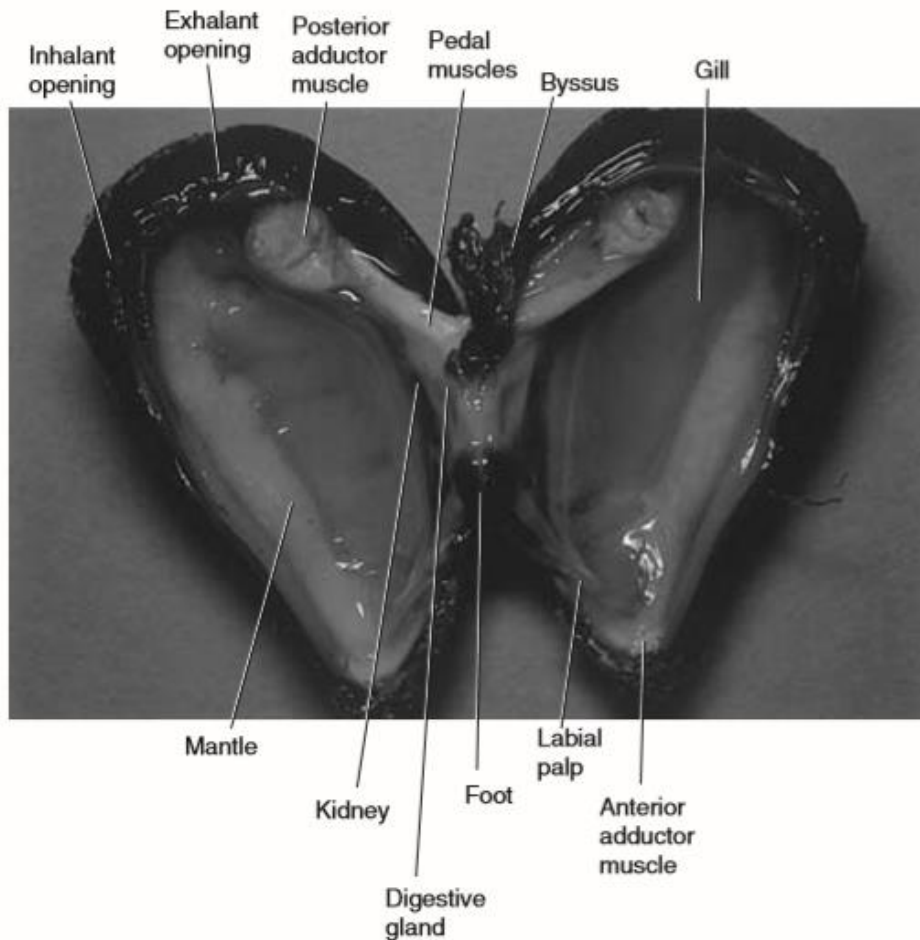


Figure 5: Photo in a sketch representing *Mytilus galloprovincialis* morphology. Adapted from [48].

The mussel's food consists of a variety of suspended particles, such as bacteria phytoplankton, microzooplankton, detritus, but also dissolved organic material, such as amino acids and sugars, ranging in size from about 10–350 μm . Nevertheless, the food particles are normally present in very low concentrations, so the mussels can preferentially select nutritive particles and specific food types and reject particles of poor nutritive value. This capacity allows them to coexist with another species and prevents the uptake of nanoparticles when present in higher concentrations. At low concentrations, all filtered particles may be ingested [48].

Once exposed to nano-sized aggregated particles and materials in the water, mussels can uptake these through the large respiratory surface of the gills or the digestive tract, being the digestive gland the tissue with privileged accumulation, increasing simultaneously with exposure duration. Once in the tissues, the nanostructures can promote several abnormalities in cellular function, leading to morphological changes, or even animal death [50, 51].

Mediterranean mussels are the main aquaculture species produced, in weight terms, in European Union, mainly in Spain and Italy. Worldwide total mussel production reached 1.9 million tons and 2.0 billion USD in 2012, and these numbers certainly increased until today [52]. So, *Mytilus galloprovincialis* are important elements of the human food chain in several countries, and plastic pollutants can define a potential risk for that consumers as the mussels become contaminated [47,50,53].

Marine mussels, such as *Mytilus galloprovincialis*, have been a model for both ecotoxicological and food safety tests, since they were proposed as sentinels' organisms of coastal waters, more than 40 years ago [51]. Their capacity to concentrate contaminants and metals in their soft tissue and their global geographical distribution, led to the beginning of mussel watch programs [52]. Over this time, bioaccumulation studies reveal to be a complex process governed by the bioavailability of the contaminant in water and suspended particles and the route of exposure [53]. Nevertheless, *M. galloprovincialis* have become a model for ecotoxicological studies, for nanomaterials like, TiO₂ [34–38, 51], ZnO [43], Ag [57], copper (Cu) and copper oxide (Cu₂O) [58], and nanoplastics [59], and also for microplastics [60] and pharmaceuticals [61], for example.

The increasing use of marine mussels as bioaccumulation models for different nanomaterials, especially, engineered nanomaterials, verified on last year's is triggered by the need to understand possible implications for human health.

II. Materials and Methods

1. Chemicals and reagents

Hydrogen peroxide (H_2O_2 , >30% w/v), hydrochloric acid (HCl, trace metal grade, 34 – 37 %), sulfuric acid (H_2SO_4 , 96 %, extra pure, solution in water), nitric acid (HNO_3 , trace metal analysis, 67-70%) and Trizma® base (Tris) were obtained from Fisher Chemical (Lisbon, Portugal). Neutrased® (0.8 U/g) was acquired from Novozymes® (Bagsvaerd, Denmark). Calcium chloride (CaCl_2 , $\geq 93\%$, anhydrous, granular) and diethylene glycol ($\leq 100\%$), standards for ICP (silver, titanium and zinc), were provided by Sigma-Aldrich (Lisbon, Portugal). Tetramethylammonium hydroxide (25% w/w, aqueous solution) was bought from AlfaAesar® (Kandel, Germany).

Silver powder coated with polyvinylpyrrolidone (25% silver, 75% polymer) and titanium oxide nanopowder (Rutile 99.5%) were provided by Skyspring Nanomaterials, Inc. (Houston, TX, USA). Colloidal suspension of zinc oxide nanoparticles in diethylene glycol (1.0 ± 0.2 %w/w) was acquired from Gruppo Colorobbia® (Vinci, Italy).

Ultrapure water ($18.2\text{M}\Omega$ cm at 25 °C) was used for sample preparation.

Saltwater was prepared mixing marine salt provided by ICA with deionized water, reaching a final salt concentration of ± 33 ppm. The salinity was verified using a V²refractometer from TMR® aquarium.

2. Engineered nanomaterials dispersion

All the engineered nanomaterials (ENMs) suspensions were prepared in order to obtain the best dispersion possible on saltwater. For ZnO NPs there was no need to sonicate, for the others ENMS, after testing different options, the chosen techniques and conditions are those presented on Table 1. Ultrasonication with probe was performed with a disintegrator ultrasonic S-450, from Branson.

For all the ENMs, two suspensions were prepared at final concentrations in the aquariums of 1 mg/L (suspension I) and 0.1 mg/L (suspension II), respecting the OECD regulation, with maximum concentration of 0.1 mL/L solvent.

Table 1: Sonication conditions for ENMs dispersion in solution to be applied in mussel bioaccumulation study.

ENMs		TiO ₂	Ag
Type of sonication		Ultrasonication with probe	
Time (min)	Suspension I	40	5
	Suspension II	10	3
Pulse ON (sec)		30	
Pulse off (sec)		5	
Amplitude (%)		70	30

3. Dynamic Light Scattering

Dynamic light scattering (DLS) is a technique widely used to determine the size and dispersity of the particles in suspensions and colloidal solutions whose size is too small for optical microscopy analysis and too big for electron microscopy analysis, but can also be used in other specific properties depending on the chosen detector [62,63]. The DLS technique is based on the principle that particles have random movement (Brownian motion) caused by the collision forces between the particles and the solvent molecules, so smaller particles move faster than bigger ones [62,63]. Since the movement depends on temperature, viscosity, concentration and size, it is crucial to guarantee stable conditions to get reliable results. When the sample is irradiated by a laser beam, the light scattering by the Brownian motion reflects particles size and shape. The processing of these aleatory fluctuations is done from a correlation function that has an exponential decay over time [62]. Based on the mobility of particles in suspension when an electric field is applied, it is possible to measure the zeta potential value that represents the electrostatic potential at the potential of a shear, generally called the particle surface charge. Typically, zeta potential values of ± 30 mV are representative of stable particles, values $>+30$ mV and <-30 mV, are associated to more instable particles that easily form aggregates [64]. For all the ENMs, both suspensions I and II were analyzed.

The samples were read five times in a 173° angle in a macro standard PMMA 4,5 mL cuvette, using a Dynamic Light Scattering System SZ-100, from Horiba (Dias de Sousa).

4. Inductively Coupled Plasma - Optical Emission Spectrometry

Previously, trace metals were analyzed using flame atomic absorption techniques, that despite being almost interference free, it requires intensive labor, since only one element is analyzed at each time, and

colorimetric techniques, which were both unworkable and subject to interferences. Commercial inductively coupled plasma - optical emission spectrometry (ICP-OES) instruments became available in 1974, responding to a needed efficient trace metal analysis in environmental samples with a set of convenient characteristics like high precision, detection limits and a wide linear range. ICP coupled to OES has become the dominant technique for rapid spectroscopic multielement trace metal analysis [65, 66].

The ICP is a partially ionized gas, normally Argon (Ar), produced in a quartz torch using radio frequency power supply, in which ions (Ar^+ and Ar^{2+}) and neutral Ar atoms coexist. Typically, the samples are nebulized into the center of the plasma. Optical emission spectrometry is a method, sensitive and selective that can trace several elements sequential or simultaneously, based on element's radiation emissions ionized in Ar [67].

In this work, ICP-OES was used to quantify of metals retained in the mussel flesh after exposure to metallic nanoparticles. Every sample was measured in triplicate and each replica was analyzed three times for seventy seconds. The wavelengths were chosen considering the element: 243 nm for Ag, 334, 336 and 337 nm for Ti, and 206 and 213 nm for Zn. In each quantification run was used a 11-point external calibration curve from 0 to 2 mg/L for all the elements (figure 6).

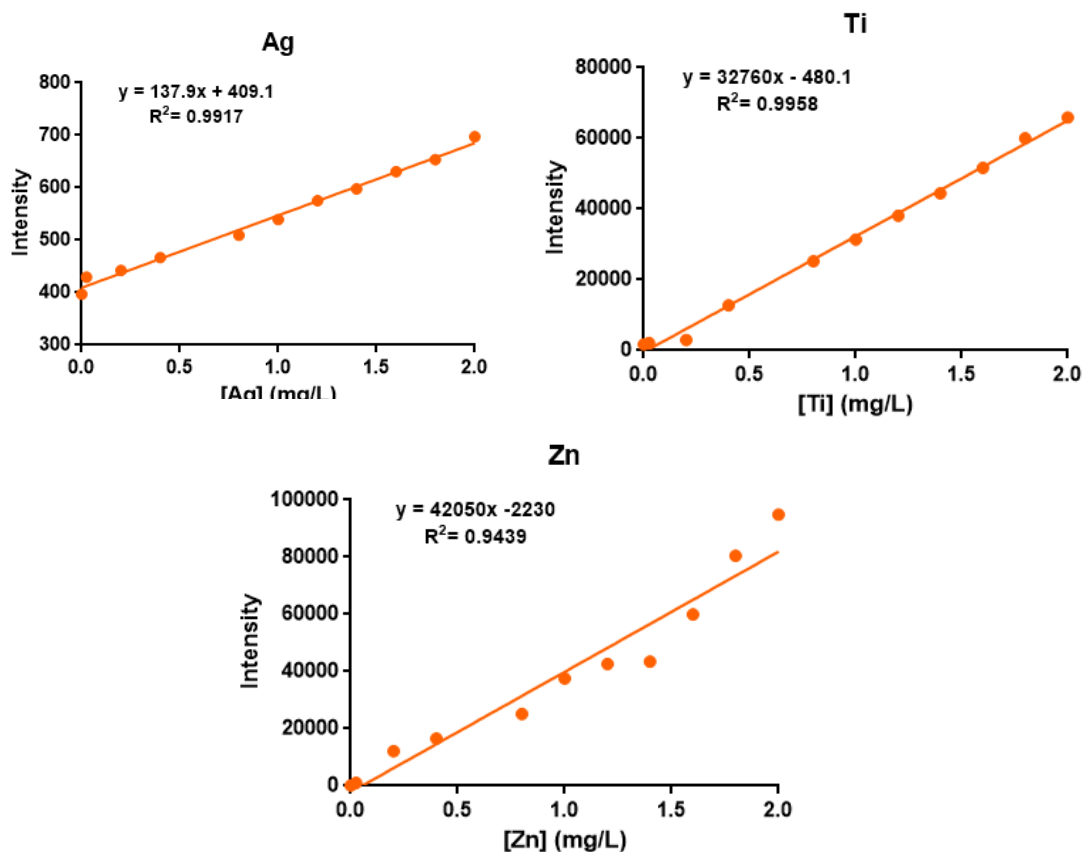


Figure 6: ICP-OES calibration curve for all the ENMs. 11-point external calibration curve from 0 to 2 mg/L (ppm) for Ag, TiO₂ and Zn.

For this quantification, a spectrometer ICPE-9000, from Shimadzu, was used with the conditions in Table 2.

Table 2: ICP-OES conditions

Radio Frequency Power (kW)	1.20
Plasma Gas flow (L/min)	10.00
Auxiliary Gas flow (L/min)	0.60
Carrier Gas flow (L/min)	0.70
View Direction	Axial
Sensitivity	Wide Range
Exposure time (s)	30
Solvent Rinse Time (s)	70
Sample Rinse Time (s)	70

The limit of detection (LOD) and limit of quantification (LOQ) for the instrument and method were calculated by the equations: $LOD = S_b + 3SD_b$ and $LOQ = S_b + 10SD_b$ equations. Where S_b is the ICP-OES signal for of blank samples and SD_b the standard deviation of blank intensities. LOD value was ≈ 0.01 mg/L for

Ag; ≈ 0.09 mg/L for Ti and ≈ 0.16 mg/L for Zn. LOQ value was ≈ 0.10 mg/L for Ag; ≈ 0.10 mg/L for Ti and ≈ 0.18 mg/L for Zn.

5. Sample preparation: mussels' tissue digestion and ENMs dissolution

Four mussels from each condition and time point, the organic matter was oxidized with a concentrated acid mixture $\text{HNO}_3:\text{H}_2\text{O}_2,7:3$ V/V (35:15 mL), over 3 h at 80 °C and left overnight shaking. For nanoparticles dissolution, 10 mL of concentrated HNO_3 (trace metal analysis, 67-70%) was added to silver and zinc oxide and 5 mL of HNO_3 and 10mL of H_2SO_4 to titanium oxide. The samples stayed at room temperature in agitation during approximately 4h, for Ag and ZnO, and overnight, for TiO_2 , and subsequently the volume was evaporated, in a hot plate, with gradually increasing temperatures, from 150 °C to 200 °C, as needed, until a final volume of ± 15 mL. This final solution was stored at 4 °C until analysis with ICP-OES [67 – 70]. This protocol was based on the Standard Method 3030G [67].

In order to improve the organic matter oxidation, two different protocols were tested, adding an extra oxidation step with alkaline or enzymatic digestion, before adding H_2O_2 . For alkaline digestion, the tetramethylammonium hydroxide (TMAH) was chosen added in a 20:1 ratio (mL solvent: g mussel) and left overnight shaking. For enzymatic digestion, 1.5 mL of Neutrase® (0.8 U/g) was added to four mussels mixed with 50 mL of 0.05 M Tris-HCl 0.01 M CaCl_2 buffer (pH 7.5) and left shaking during 6h at 50°C [71 – 74]. For both sample preparation treatments (with or without the extra pre-step of organic matter digestion) recovery rates were calculated by quantifying the metal in a sample of mussel flesh spiked with a known concentration solution of ENM.

6. Transmission Electron Microscopy

Over the last decades, transmission electron microscopy (TEM) has played a key role on scientific understanding of materials' properties. A TEM image is formed by signal radiating from the sample when electron beam interacts with the specimen. With the current generation of electron microscopes, it is possible to obtain a spatial resolution of approximately 0.05 nm, which means that small differences in structure and composition, and even atomic structure of materials, can be observed [75]. However, to obtain most high-resolution stable observations it is necessary to overcome drift, charging, mechanical

instabilities, stray fields, beam damage and so on, and that can be a constant handicap, particularly for non-conductive materials [75].

In TEM, apart from imaging and diffraction techniques, it is possible to characterize the structural, chemical and physical properties of materials with different coupled spectroscopy methods such as energy-dispersive X-ray (EDX) [75]. Therefore, EDX was used to corroborate samples' chemical composition.

Mantle and hepatopancreas samples were finely cut and fixed with 2% paraformaldehyde, 2.5% glutaraldehyde in sodium cacodylate buffer (0.1M, pH 7.2) and left to incubate overnight at 4°C. After, samples were washed three times with 0.1 M cacodylate buffer and post-fixed with 1% osmium tetroxide in the same buffer, overnight at 4°C. The osmium residues were repeatedly removed with washes of 0.1M sodium cacodylate buffer and the samples were dehydrated with increasing concentrations of ethanol (50%, 70%, 90%, 95% and 100%), ending with 100% propylene oxide. Infiltration was made by draining the excess of propylene and replacing it by a 3:1 propylene oxide: embedding resin (EMBed-812, EMS) mixture followed by 1:1, 1:3, and finally 100% resin, waiting at least 2h between each replacement. Each sample was transferred to a dry silicon mold which was then filled with embedding resin and left to cure at 60°C for 3 days [76]. Lastly, the blocks were trimmed and prepared with a regular ultramicrotome glass knife and cut into ultrathin 70 nm thick sections with a diamond knife (Diatome ultra, 35°), in a PowerTome PC ultramicrotome from RMC Boeckeler. For control pictures, a drop of every ENM was placed in the grid and left to dry for at least 24 h.

7. Scanning Electron Microscopy

The scanning electron microscope (SEM) is one of the most versatile instruments available for the examination and analysis of size, morphology, surface texture and roughness, and chemical composition [77, 78]. A SEM image is formed by a focused electron beam that scans over the surface area of the specimen and interacts with it, taking advantage of the short wavelengths of electrons focused by electromagnetic lenses, the SEM can achieve high-resolution imaging with a large depth of field that confers a three-dimensional appearance to the images [77, 78]. In nanotechnology, SEM has an important role in the research of all types of nanomaterials and bionanomaterials, from nanoparticles and nanostructured semiconductors/thermoelectric materials to nanofibrous and nanocomposite scaffolds for bone and tissue engineering, observing their morphologies and confirming their orientations [78]. EDX

spectrometry combined with SEM allowed the determination of the chemical composition of the particles present on the samples [79].

The bombardment of samples by relatively high-energy electrons quickly results in a build-up of negative charge so, since the mussel shell is not electrically conductive, the samples were sputter-coated during 30' with zirconia, a conductive material. This electrically conductive coating provides a ground plane for the electrical field and can also, somehow, protect the sample from physical damages caused by the specimen heating due to radiation [77, 78]. The samples were fixed to the holder with copper tape.

For control pictures, clean mussel's shells were spiked with a 100 mg/L concentration solution of all the ENMs and left to dry.

8. Mussels maintenance and exposure

Adult mussels, *Mytilus galloprovincialis*, were obtained from Falcamar (Labruge, Portugal), already depurated (as commercial). The animals, 46 *per* aquarium, were acclimated to laboratory conditions for at least one week. They were maintained at $18\text{ }^{\circ}\text{C} \pm 2\text{ }^{\circ}\text{C}$ with a 14 / 10 h light/dark photoperiod and were nourished with commercial food adequate for filter feeders (NTLabs) every other day. Each aquarium was individually aerated and filled with synthetic seawater that was periodically renewed. The water quality was controlled by monitoring various physicochemical parameters, such as salinity, temperature, conductivity, and oxygen concentration, using a multiparametric probe (HI98194), from Hanna Instruments®.

After the acclimation period, the water quality control was maintained, and the animals were nourished with living cultures of *Chlorella vulgaris* (1×10^5 cell/mL). Over 28 days, in 3 replicates *per* experimental condition, the animals were exposed to ENMs: TiO₂, Ag and ZnO to the nominal concentration of 0, 0.1 and 1 mg/L, respecting the OECD regulation, in the feeding microalgae culture once *per* week. The solutions were always freshly prepared by dilution series and were sonicated for a better dispersion according to the conditions, presented on Table 1. Additionally, animals were exposed to 0.1 mL/L of diethylene glycol as solvent control of ZnO.

Three replacements of water were made every week, two of 25% and one of 100% and, in the latter, the ENMs solution was renewed. The ENMs solutions were pre-mixed with *Chlorella vulgaris* before being added to each aquarium.

The soft tissue of four mussels were collected after 24 h, 7, 14, 21 and 28 days of exposure (T0, T1, T2, T3 and T4, respectively) and stored at $-80\text{ }^{\circ}\text{C}$ until being used for ICP-OES. In the final sampling time (28th day), one animal was collected of each experimental condition replicate for the shell imaging in SEM, and three samples of mantle and two samples of hepatopancreas were processed for TEM analysis.

9. Statistical analysis

In order to detect differences among ENMs concentrations in the overall survival of mussels, a chi-square test was conducted with the observed values for each test condition, analyzing each timepoint separately.

Multivariate analysis of variance (MANOVA) test was conducted to understand the bioaccumulation of the ENMs in mussels at different concentrations, with a level of significance of 0.05.

III. Results

1. Ecotoxicity

I. Survival

The mortality was checked daily in all the replicates from all the conditions. During the 28 days of exposure to Ag, TiO₂ and ZnO no significant effects on the survival rate were observed in any experimental condition ($\chi^2 = 0.005$; $df = 8$; $P = 1$ for Ag, $\chi^2 = 0.119$; $df = 8$; $P = 1$ for TiO₂ and $\chi^2 = 0.339$; $df = 12$; $P = 1$ for ZnO; Figure 7).

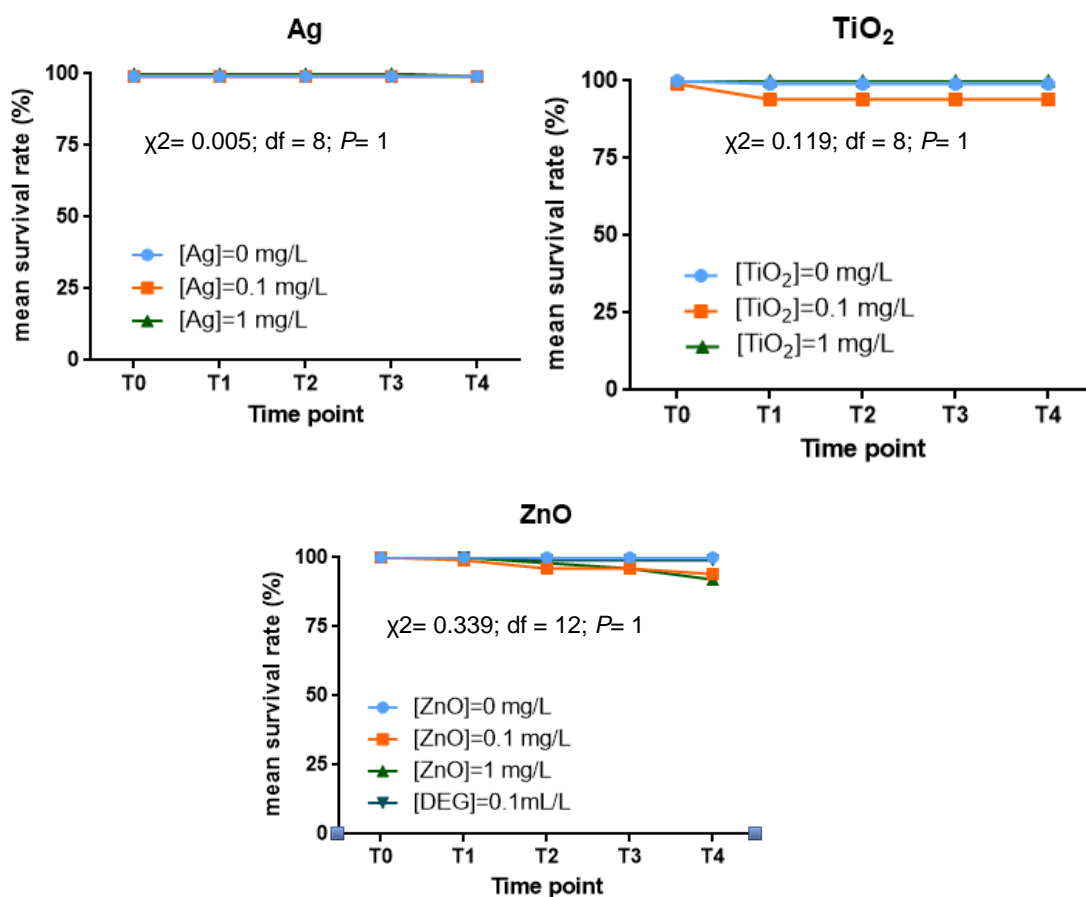


Figure 7: Evaluation of mortality rate for different ENMs concentrations in saltwater after 24 hours, 7, 14, 21 and 28 days of exposure (T0, T1, T2, T3 and T4, respectively) of exposure. The statistical data was obtained by chi-square test.

As expected, no toxicity was observed during the whole length of the bioaccumulation experiments as the concentrations of ENMs used are low, consistently with their predicted environmental concentration (PEC): 0.03 µg/L for Ag NPs, 7µg/L for TiO₂ NPs [79] and 1.26 µg/L for ZnO NPs [80].

These results agree with prevision studies, where the same concentrations were tested in marine mussels in different exposure forms and no significant direct lethal effects were found after 28 days for any of the ENMs [38,43,81].

II. Mussels morphometric parameters

For all the ENMs, no significant differences between control and treated groups were observed in all the mussel's morphometric parameters, during the 28 days of exposure.

The length of the mussel's shell (M1, Figure 8) mean values were 7.02 ± 0.10 cm for Ag, 6.89 ± 0.38 for TiO₂ and 7.44 ± 0.22 cm for ZnO. The width of the shell (M2, Figure 8) mean values were 3.45 ± 0.04 cm for Ag, 3.29 ± 0.20 for TiO₂ and 3.57 ± 0.15 cm for ZnO. The total weight mean values were 25.48 ± 0.99 g for Ag, 25.41 ± 2.99 g for TiO₂ and 29.43 ± 2.45 g for ZnO. The flesh weight mean values were 7.031 ± 0.83 g for Ag, 6.07 ± 1.11 g for TiO₂ and 7.70 ± 0.77 g for ZnO.

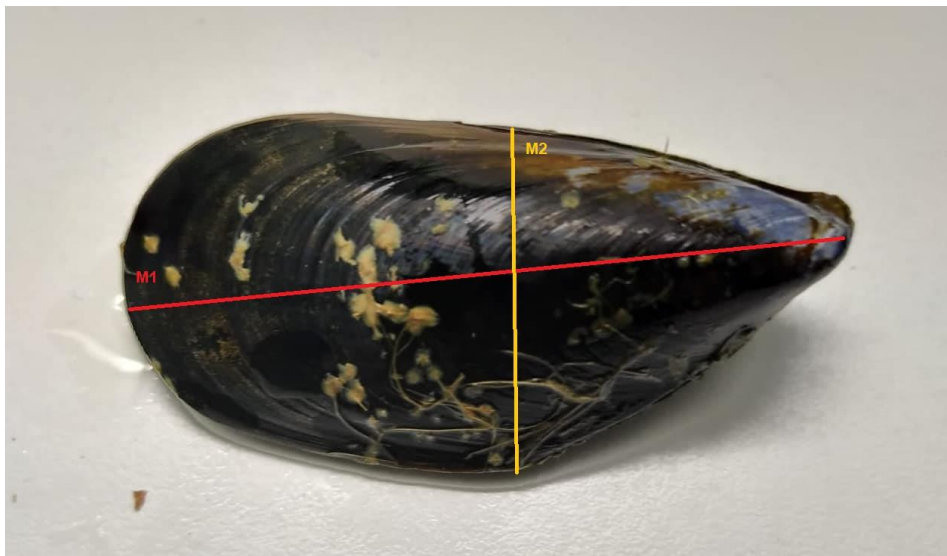


Figure 8: Photo of a closed *Mytilus galloprovincialis* mussel with a sketch representing morphometric measurements, length of the mussel's shell (M1) and width of the shell (M2).

All the evaluated morphometric parameters are in accordance with the mean values found in the *Mytilus galloprovincialis* cultures [48].

2. Physicochemical seawater parameters

For all the engineered nanomaterials, no significant differences between control and treated groups were observed in any of the physicochemical parameters, during the 28 days of exposure.

The pH mean value was 8.39 ± 0.15 for Ag; 7.92 ± 0.27 for TiO₂ and 8.17 ± 0.12 for ZnO. The percentage of dissolved oxygen (% LDO) mean value was 81.12 ± 1.20 for Ag; 84.76 ± 9.63 for TiO₂ and 83.79 ± 4.69 for ZnO. Regarding concentration of dissolved oxygen ([DO] mg/L), the mean value was 5.98 ± 0.33 for Ag; 7.34 ± 0.27 for TiO₂ and 6.07 ± 0.36 for ZnO. Saltwater conductivity mean value was 51.37 ± 0.63 for Ag; 48.33 ± 4.68 for TiO₂ and 54.72 ± 4.29 for ZnO. The salt concentration (PSU) mean value was 33.96 ± 0.40 for Ag; 31.96 ± 1.00 for TiO₂ and 36.37 ± 3.12 for ZnO, which can be considered normal values since open oceans salinity varies between 32 PSU and 38 PSU, with an average of 35 PSU [82]. The saltwater temperature mean value was 19.50 ± 0.43 for Ag; 17.68 ± 0.48 for TiO₂ and 20.04 ± 0.54 for ZnO.

All the evaluated physicochemical parameters values are close to those found in the *Mytilus galloprovincialis* cultures [48].

3. Optimization of ICP-OES sample preparation: mussels' tissue digestion and ENMs dissolution

For ICP-OES sample preparation, a standard digestion protocol was followed but low recovery rates were obtained (Table 3), compared with other studies [67 – 70]. So, in order to improve the recoveries throughout better organic matter degradation, enzymatic and alkaline digestions steps pre-acidic digestion [71 – 74] were tested, separately, and the recoveries increased for the enzymatic (Table 3).

Table 3: Recovery rate values from ICP-OES samples digestion protocols, with and without enzymatic digestion step with Neutrase®.

	Recovery rate (%)	
	Without enzymatic digestion	With enzymatic digestion
Ag	45.00 ± 1.00	68.60 ± 10.22
TiO ₂	4.11 ± 0.04	25.58 ± 1.82
ZnO	31.85 ± 0.07	34.23 ± 0.77

Despite both used protocols, with and without enzyme, very similar to those used in previous studies, recovery rates were lower. This could result from the fact that the digestion was not performed in a closed vessel in a microwave, which increased the risk of ENMs loss and without the possibility of reaching high pressures that help to dissolve the ENMs [67, 69, 71, 73, 74].

Although the recovery rates are still not optimal ($\geq 80\%$), the addition of an extra step in degradation of organic matter with Neutrase® showed a considerable improvement comparing with the acidic digestion original protocol, which can be explained by the fact that H₂O₂ and HNO₃ become available to dissolve the ENMs.

In the case of TiO₂ nanoparticles, the recovery rate could be improved by adding hydrofluoric acid (HF), but that was avoided due to its high risk for manipulation that requires expensive and time-consuming safety precautions added to corrosive effects in ICP-OES equipment if HF are not neutralized before being injected in the system [83].

For ZnO nanoparticles, the recovery rate is far from the 80% probably due to the presence of the diethylene glycol that protects the ZnO NPs from the HNO₃ during the digestion, creating emulsions and reacting with the acid, being oxidized [84].

The alkaline digestion step, with TMAH, was only tested for TiO₂ NPs obtaining a 11.98 % recovery rate, only slightly better than with the acidic digestion alone. So, TMAH digestion was not considered an option given that the improvement was not enough to justify moving forward with a protocol that would imply an extra overnight step.

The following presented quantification results were obtained using the enzymatic digestion.

4. Silver nanoparticles stability and bioaccumulation

The obtained hydrodynamic size of the Ag NPs in the mussel's seawater measured was 43.34 ± 1.46 nm for suspension I and 36.50 ± 1.68 nm for suspension II, with a PDI value of 0.53 ± 0.06 and 0.93 ± 0.04 , respectively. These results can be explained by a small aggregation and the water layer around the particle, since the particles seem to have a real size of 15 nm by TEM analysis [44].

Analyzing ICP results (Figure 9) it is possible to observe a slight increase on Ag concentration from T0 to T4 ($F(8, 30) = 2.77, P = 0.02$). It is also worth to note that the mussels contain and significant initial concentration of Ag (between 7.7 to 10.9 $\mu\text{g/g}$), amounts that can be explained by the nano-silver that has been found in rivers all over Europe. These particles can easily reach the oceans and became part of mussel's natural habitat and be internalized by them [85].

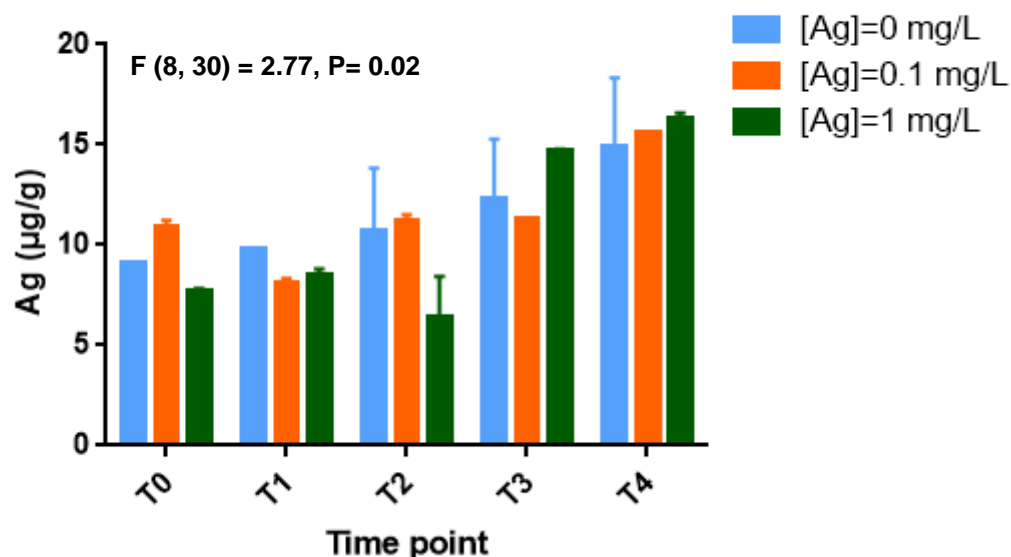


Figure 9: Silver (Ag) quantification by ICP-OES, in soft tissue mussel samples collected after 24 hours, 7, 14, 21 and 28 days of exposure (T0, T1, T2, T3 and T4, respectively) of exposure, from a random replica of each condition ($F(8, 30) = 2.77, P = 0.02$).

In related studies, the basal amount of silver (mass of silver in T0) is not considered since the goal is to calculate the bioaccumulation from the moment that the first spike is made. In this study, commercial mussels were used, and it is interesting to observe that significant amounts of Ag are found, even after depuration for several days.

During the 28 days of treatment, 310 $\mu\text{g/g}$ of Ag NPs in 1 mg/L concentration were added to the aquariums. So, observing the results, and considering the recovery rate (approximately 70%) it is possible

to calculate that only 5% of the Ag added was accumulated in the mussel flesh, so probably, high amount of silver was excreted by the mussels.

Comparing each treatment, the biggest increase is detected in the highest exposure concentration (1 mg/L), which is logical since more nanoparticles were added to the aquariums and is concordant with electron microscope results. T4 results for 0.1 mg/L and 1 mg/L are very similar (around 16 $\mu\text{g/g}$), it can be explained by the highest pre-existent amount of silver (T0) in mussels from 0.1 mg/L treatment but it can also mean that mussels are only capable to internalize a limited amount before starting to suffer internal damage (for example by ROS production) and losing the capacity to eat properly. This variation in the results meet those observed in similar studies, where almost 30 $\mu\text{g/g}$ (mussel's dry weight) were found in mussel's digestive gland after 15 days of exposure to 10 $\mu\text{g/L}$ of Ag NPs renewed every 12 hours [81].

In accordance to ICP results, TEM results (Figure 10) suggest that there was some internalization of Ag nanoparticles in the mussel's hepatopancreas tissue. In the mussel that was not exposed to AgNPs (Figure 10A) it was not possible to observe any kind of particles, while in the one that was exposed to 1 mg/L of AgNPs (Figure 10B) their presence is clear. The nanoparticles appear to be aggregated (Figure 11), but the most individual elements exhibit an average diameter of 23 nm, which is in accordance with the expected size for the tested silver nanoparticles, since the expected diameter is 15 nm [44]. In Figure 11, it is possible to observe crystalline planes with around 0.2 nm between them while in Figure 12, stock silver nanoparticles only dispersed in ultrapure water, present a distance between crystalline planes around 0.11 – 0.17 nm. Both fringe spacings of lattices found were in the range reported in released works, where is shown that this value depends of what is the silver crystal's plane observed in the picture [86].

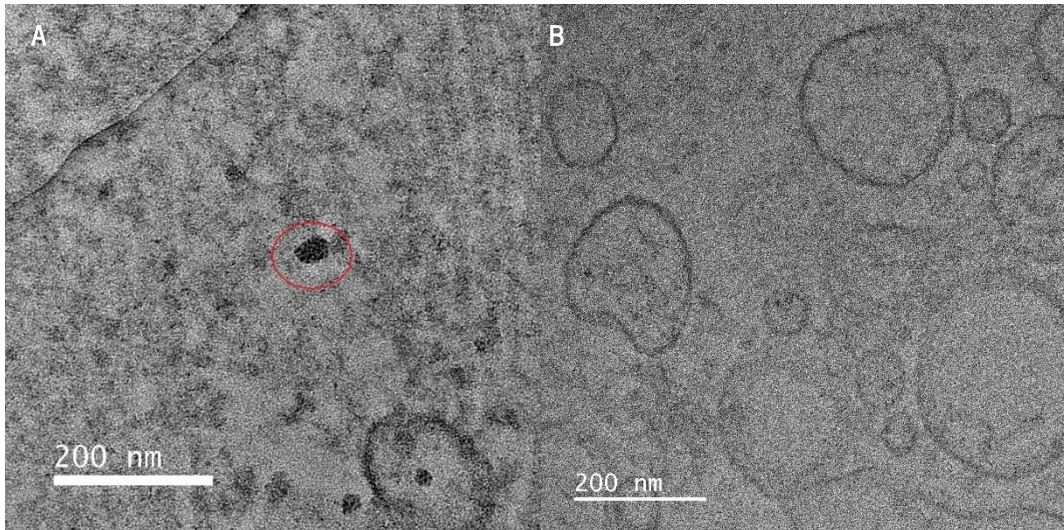


Figure 10: TEM picture of hepatopancreas tissue extracted from a mussel exposed to 0 mg/L (A) and 1 mg/L (B) of silver nanoparticles for 28 days (50 000x magnification; 200 kV voltage). Within the red circle is possible to observe a nanoparticle aggregated.

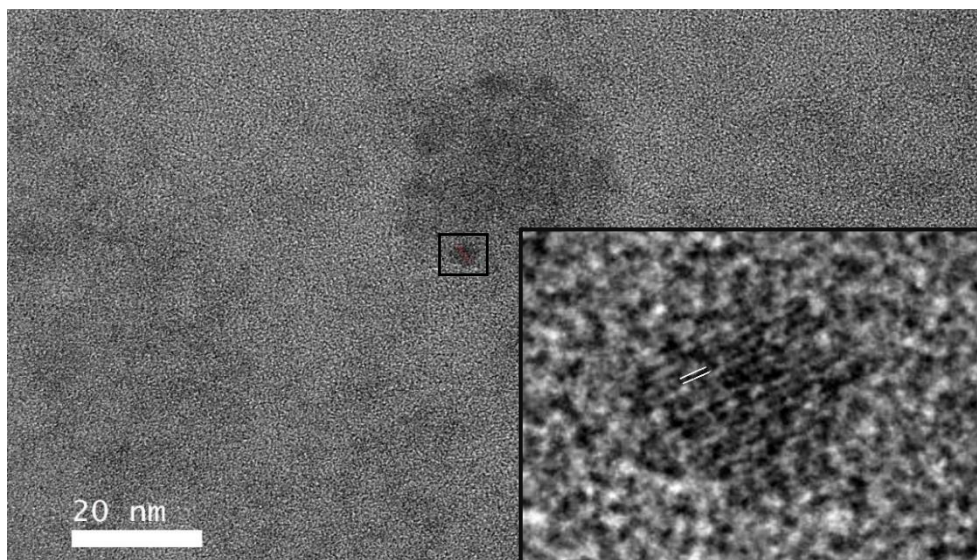


Figure 11: TEM picture of hepatopancreas tissue extracted from a mussel exposed to 1 mg/L of silver nanoparticles for 28 days (300 000x magnification; 200 kV voltage). Within the square is possible to observe a nanoparticle, supposedly silver, and its crystalline planes.

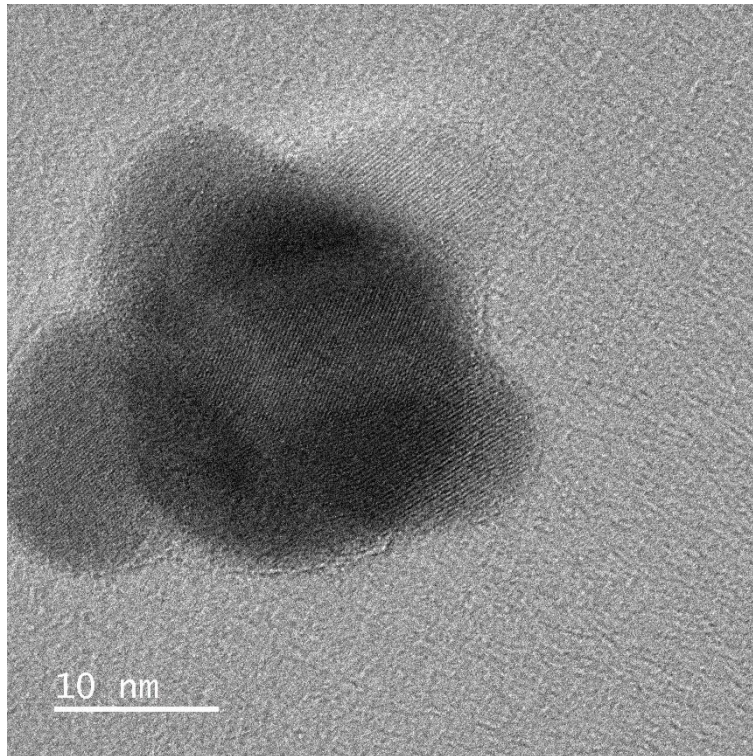


Figure 12: TEM picture of grid spiked with a silver nanoparticles solution (1 000 000x magnification; 200 kV voltage). It is possible to observe a silver nanoparticle aggregate and the nanoparticles crystalline planes.

Despite the experiment was not carried out in sterile conditions and the mussels were previously exposed to all kinds of materials on their natural habitat, the fact that crystalline planes from the mussel's sample (Figure 11) correspond to the ones from the AgNPs solution (Figure 12) highly suggest that mussels internalized the silver nanoparticles during the feeding process and these particles were incorporated into the hepatopancreas tissue, agreeing with previous studies [81].

Mantle tissue from the same mussel was also analyzed via TEM but no conclusive pictures were obtained.

The shell of a mussel exposed to 1 mg/L silver nanoparticles was analyzed with SEM and some nanoparticles were imaged (Figure 13)

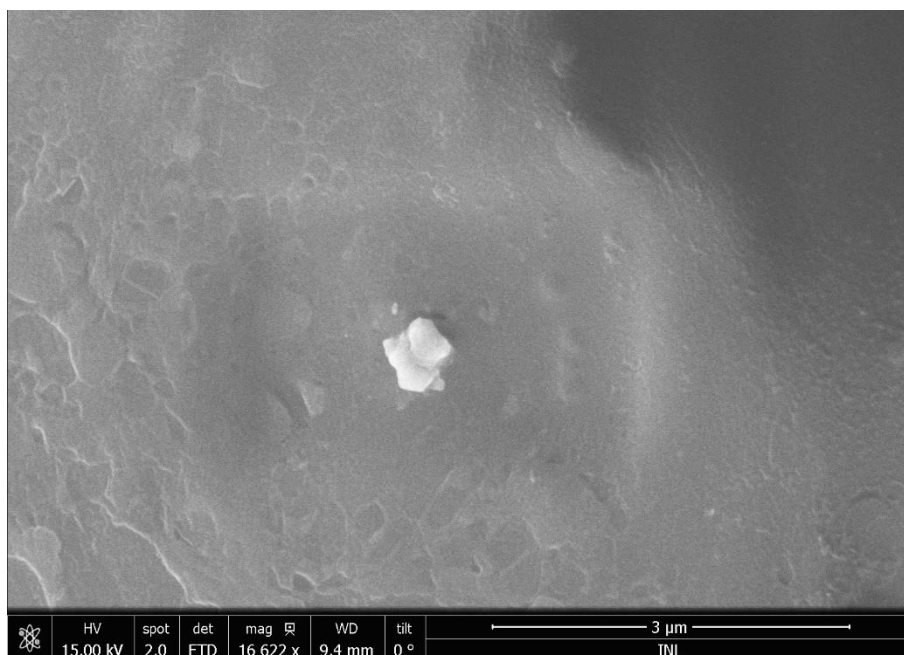


Figure 13: SEM picture of the outer shell surface belonging to a mussel exposed to 1 mg/L of silver nanoparticles for 28 days. In the picture it is possible to observe some nanoparticles in the shell surface.

In order to confirm the chemical composition of these nanoparticles, an EDX analysis was performed all over the shell surface and no traces of silver were detected. To try to understand how silver nanoparticles would look like in the shell surface, a drop of a 100 mg/L dispersion was left to dry in a clean mussel shell surface and the sample was analyzed on SEM (Figure 14). In figure 14, it is possible to observe small and shining nanoparticles that seem to match in size with the stock powder [44] and look completely different from the ones imaged in Figure 13.

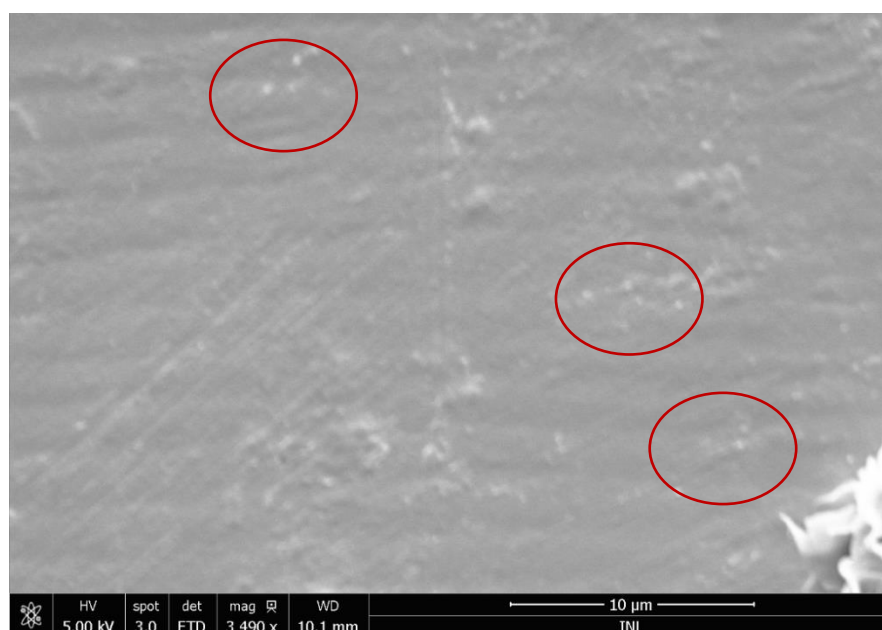


Figure 14: SEM picture of the outer shell surface with a 100 mg/L silver nanoparticles solution on the surface. In the picture it is possible to observe small and shining nanoparticles dispersed throughout the shell surface.

The overall results of these techniques indicate that a small fraction of the AgNPs are internalized by mussels during the feeding process. The internalized NPs seem smaller (around 5nm) than the ones in the stock solution, suggesting that dissolution of the primary NPs occurred. Regarding the lack of adsorption to the shell, since this analysis was not performed in previous reports [81].

5. Titanium dioxide

The mean hydrodynamic size of the TiO₂ NPs dispersed in seawater was found to be 3385.48 ± 502.7 nm for suspension I and 5168.5 ± 1436.98 nm for suspension II, with a PDI value of 1.4 ± 0.30 and 5.71 ± 3.04, respectively. These results can be explained by the tendency of TiO₂ to easily aggregate intensified by the presence of salts in the suspension [87].

Analyzing ICP results (Figure 15), there is no big difference between the mussels exposed to the three TiO₂ NPs concentrations and the unexposed, in relation to time (F (8, 30) = 4193, P< 0.0001). Given the fact that values obtained for Ti were always close to the LOQ of the ICP-OES equipment (≈ 0.09 mg/L) and that the recovery rate from digestion is low (25.58 ± 1.82 %) implies working with pretty low values, increasing the associated error.

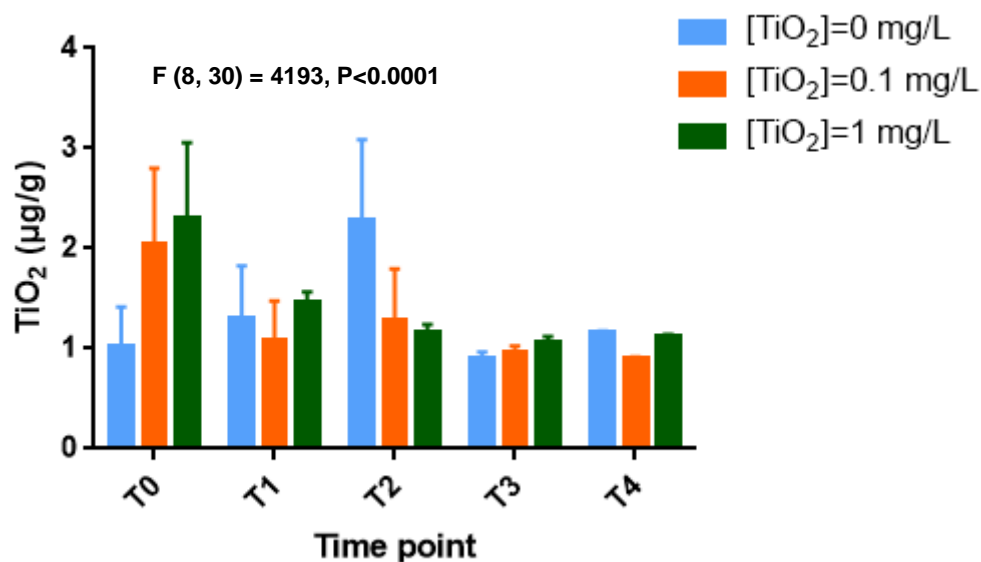


Figure 15: Titanium dioxide (TiO₂) quantification by ICP-OES, in soft tissue mussel samples collected after 24 hours, 7, 14, 21 and 28 days of exposure (T0, T1, T2, T3 and T4, respectively) of exposure, from a random replica of each condition (F (8, 30) = 4193, P< 0.0001).

On the other hand, since during the 28 days of exposure mussels get exposed to approximately 360 $\mu\text{g/g}$ of TiO_2 NPs, an ICP-OES quantifiable mass, the fact that the values quantified are always below 5 $\mu\text{g/g}$ supports the idea that, if any, the accumulation of TiO_2 is minimum, as already reported in previous works, where the authors suggest that TiO_2 NPs were transiently accumulated in the gut of mussels but not internalized, being easily eliminated via depuration [29].

Although there is no considerable TiO_2 NPs concentration variation during the 28 days of exposure, there is a TiO_2 background that persists in all samples, which seems inconsistent since the ingested NPs can, supposedly, be readily cleared from the gut. Thus, it is possible that mussels can slowly accumulate a small amount of TiO_2 NPs, from their natural habitat, in their internal organs hindering further excretion, even after weeks of depuration with clean seawater [29].

Hepatopancreas tissue sample from a mussel exposed to TiO_2 was analyzed via TEM. In the Figure 16A, it is possible to observe one black aggregate that did not seem to be organic, but the lack of resolution prevented the identification of crystalline planes or to perform EDX analysis. When compared with the hepatopancreas tissue from a mussel not exposed to TiO_2 (Figure 16B) no similar structures were noticed.

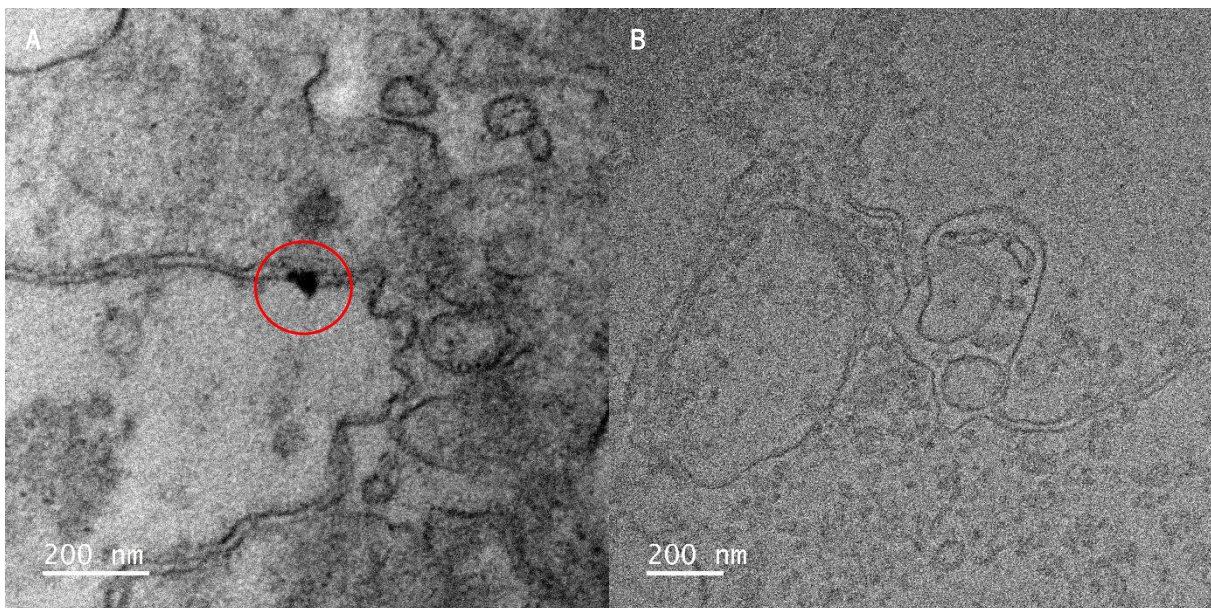


Figure 16: TEM picture of hepatopancreas tissues extracted from a mussel exposed to 1 mg/L (A) and 0 mg/L (B) of titanium dioxide for 28 days (A: 30 000x magnification and B: 15 000x magnification; both with 200 kV voltage).

A TiO_2 dispersion spiked in a TEM grid (Figure 17) was observed and the aggregates (Figure 17A) have a different appearance being possible to clearly see the nanoparticles (Figure 17B).

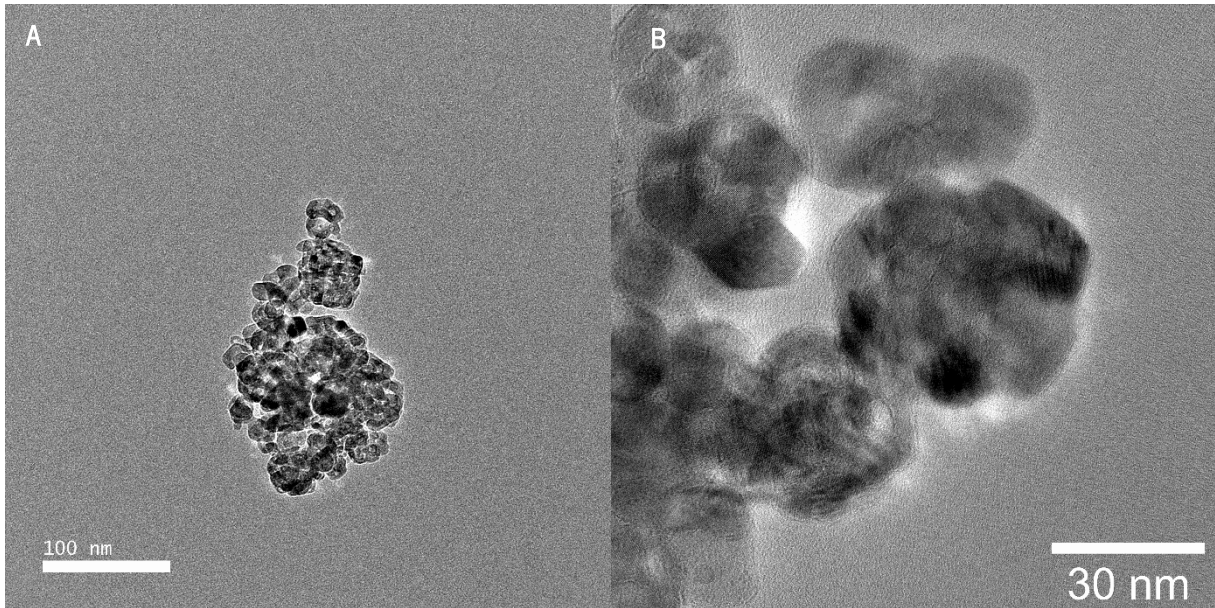


Figure 17: TEM picture of grid spiked with a titanium dioxide nanoparticles solution. (100 000x and 400 000x magnification with 200 kV voltage).

Considering the ICP-OES and the TEM results, it seems that mussels did not significantly internalize the TiO_2 NPs during the feeding process, being excreted in their feces, as reported in previous works [29].

Micro sized aggregates of particles were observed by SEM over the surface of a shell from a mussel exposed to 0.1 mg/L TiO_2 (Figure 18).

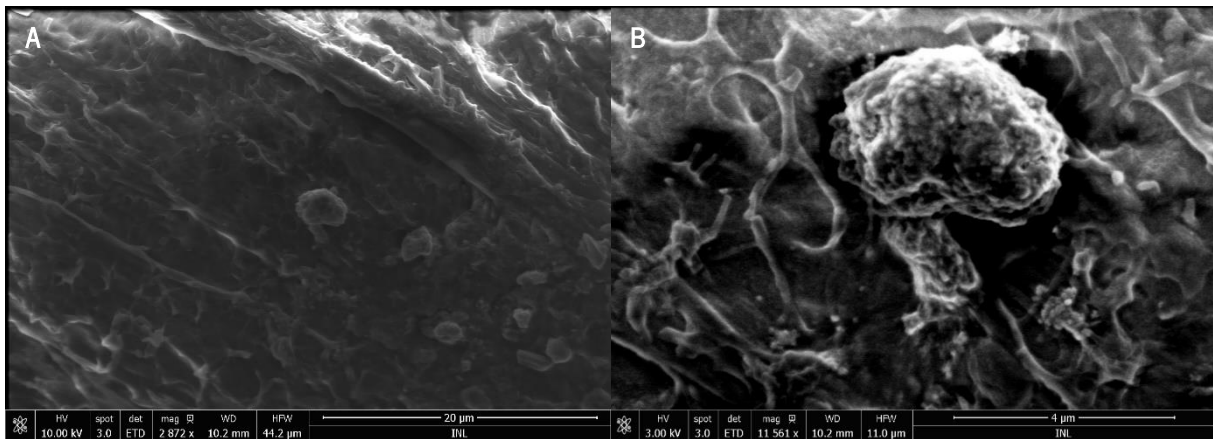


Figure 18: SEM pictures of the outer shell surface belonging to a mussel exposed to 1 mg/L of titanium dioxide nanoparticles for 28 days. In picture A is possible to observe micro sized aggregates disperse trough the surface, in B is possible to observe one presented in A but with more detail (high magnification).

To confirm if it was TiO₂, one aggregate was chosen (Figure 18B) and an EDX spectrum was plotted (Figure 19).

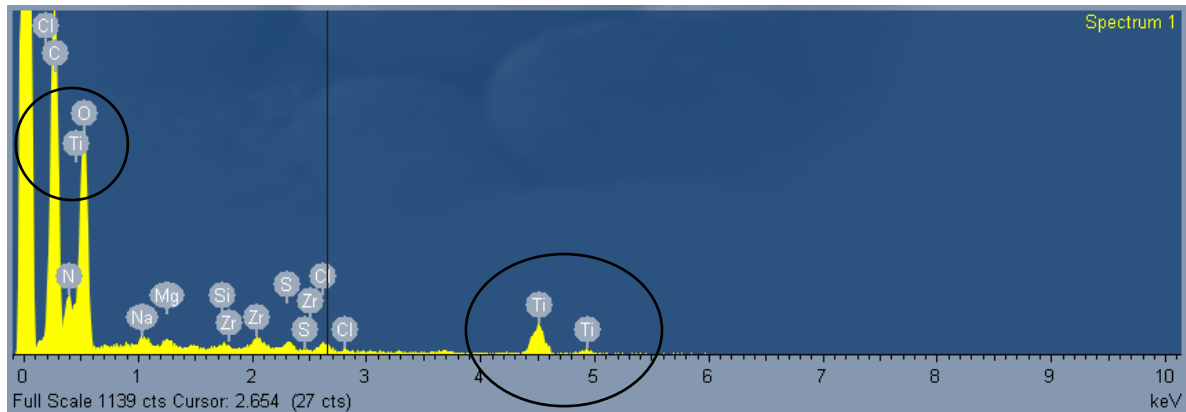


Figure 19: EDX spectrum showing chemical composition of an aggregate present on a mussel's shell surface. Within the black circles it is possible to confirm the presence of significant amount of titanium and oxygen elements.

This spectrum allows to claim that titanium dioxide nanoparticles were found adsorbed in the mussel's outer shell surface during the exposure. This is the first report showing the adsorption of TiO₂ NPs in the outer side of the shell of mussels exposed to low amounts TiO₂ NPs, indicating that this could be a significant event with relevance in seafood processing and safety, as mussels are usually cooked with their shells. This result indicates that the bioaccumulation in mussel flesh is not the only parameter that should be considering in the TiO₂ NP impact studies.

6. Zinc Oxide

ZnO NPs dispersion in seawater showed a Z-average value of 18042.78 ± 904.23 nm for suspension I and 7604.84 ± 717.27 nm for suspension II, with a PDI value of 6.46 ± 2.68 and 11.62 ± 5.70 , respectively, that reveal that particles are aggregated. The observed aggregation is probably due to the formation of emulsions due to the presence of diethylene glycol (DEG) in the dispersion, used in the ZnO NPs stock solution as solvent.

Observing ICP-OES results (Figure 20) it is possible to see that the ZnO value for the solvent control ([DEG]= 0,1 mg/L) remains stable during the 28 days of exposure. For the exposure to both concentrations of ZnO NPs, there seems to be a trend of accumulation up to T3, decreasing abruptly in T4 ($F(12, 40) = 10.71, P < 0.0001$). It was observed in the last time point that, despite not registering mortalities or changes in size and weight of mussels, some damage in the gills was observed, at least at the highest concentration (1mg/L; data not shown). If the internalization of the ZnO NPs is mediated

through the gills, this could be a possible explanation for the abrupt decay in accumulation. Decreased growth rates with increased respiration were already described in previous studies suggesting that mussels may be using energy to remove Zn from tissues, or repair damage that resulted from high concentrations of Zn instead of using this energy to produce new tissue or shell, or even to eat efficiently losing the capacity to incorporate the ZnO NPs [88].

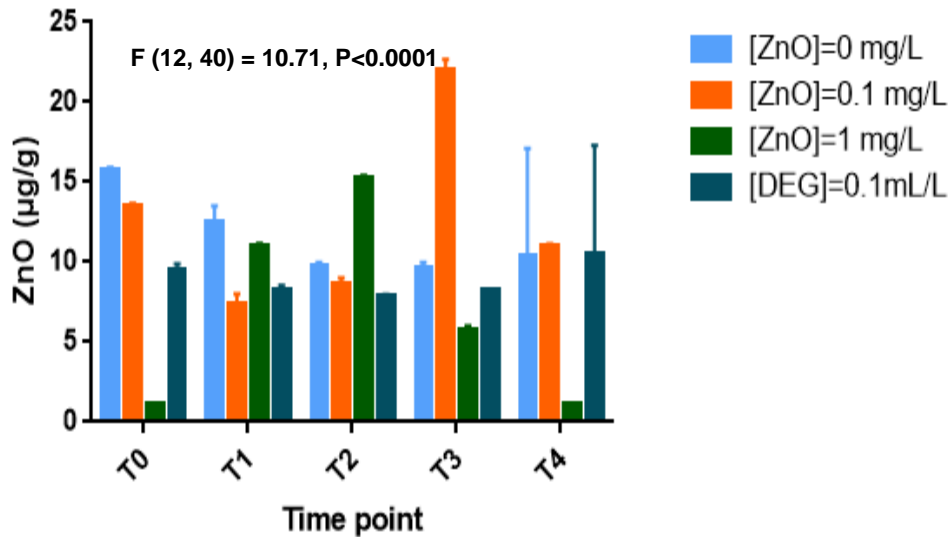


Figure 20: Zinc oxide (ZnO) quantification by ICP-OES, in soft tissue mussel samples collected after 24 hours, 7, 14, 21 and 28 days of exposure (T0, T1, T2, T3 and T4, respectively) of exposure, from a random replica of each condition (F (12, 40) = 10.71, P< 0.0001).

Like previously observed in Ag NPs, in ICP-OES results for ZnO NPs (Figure 20) it is possible to observe that the initial amount of Zn in mussels is relatively high (reach 15.7 µ/g) before exposure to nanoparticles (T0), which can also be explained by previous accumulation of ZnO NPs in the mussel's natural habitat [85]. The low recovery rate obtained (34.23 ± 0.77 %) in the digestion could also contribute to the variability observed.

Observing the SEM picture of a mussel shell exposed to 1 mg/L of ZnO NPs (Figure 21), it is possible to observe aggregates very similar to the ones found in a shell spiked with a 100 mg/L ZnO NPs solution (Figure 22).

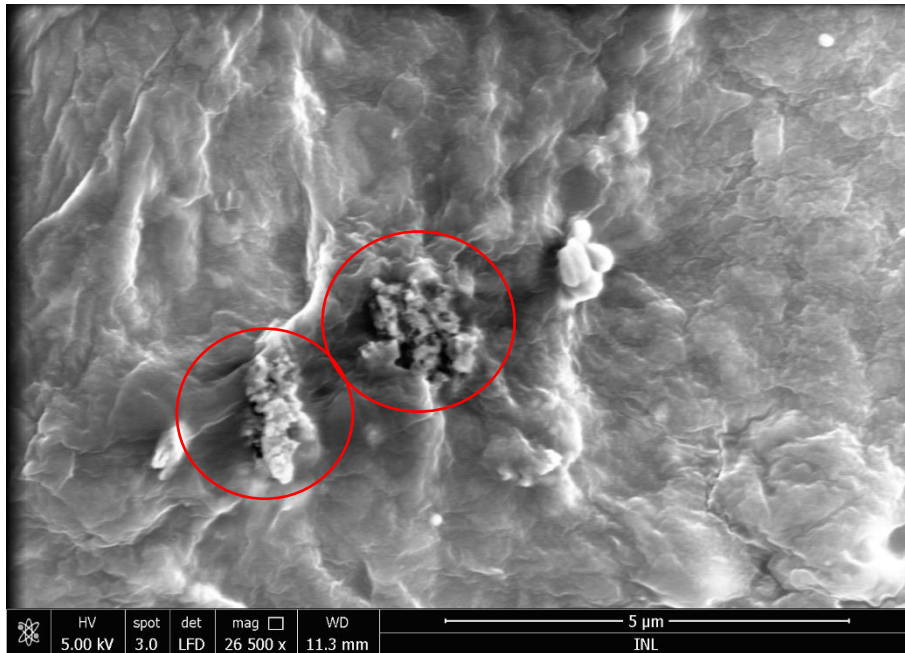


Figure 21: SEM picture of the outer shell surface belonging to a mussel exposed to 1 mg/L of zinc oxide nanoparticles for 28 days. In the picture it is possible to observe micro sized aggregates adsorbed to the surface.

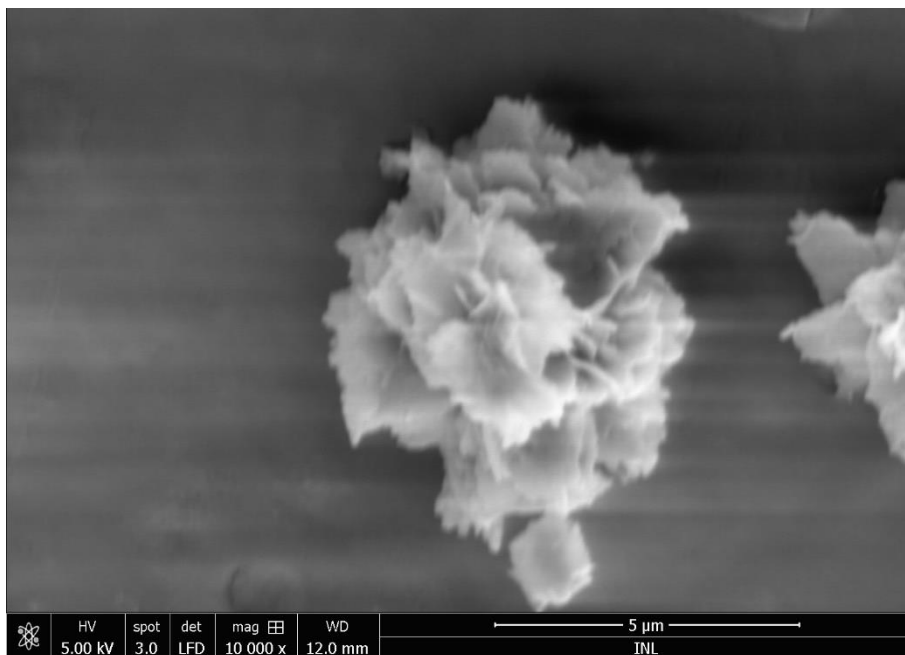


Figure 22: SEM picture of the outer shell surface with a 100 mg/L silver nanoparticles solution on the surface. In the picture is possible to observe micro sized aggregates dispersed to the surface.

In both samples it is easy to observe micro sized aggregates with amorphous morphology. This can signify that the particles not internalized by the mussel stick to the shell's surface. Like in the others ENMs, no previous studies reported this type of results.

IV. Conclusions

The digestion procedure for quantification of metallic nanoparticles accumulated in mussels using ICP-OES was optimized adding a pre-step of enzymatic digestion using Neutrase®, leading to an increased recovery rate for ENMs, getting and improvement of 20%; 68.60 ± 10.22 % for Ag NPs, 25.58 ± 1.82 % for TiO₂ NPs and 34.23 ± 0.77 % for ZnO NPs.

Up to 1 mg/L of commercial TiO₂, Ag or ZnO NPs used for bioaccumulation assays in *Mytilus galloprovincialis* mussels by feeding did not induce mortality in mussels during the 28 days exposure.

No significant amount of TiO₂ NPs was found in mussel's liver nor in mantle after the full bioaccumulation assay as observed by TEM imaging, and no significant amount of Ti was accumulated as quantified by ICP-OES, indicating that TiO₂ NPs are not accumulated and internalized by mussels, as already reported in previous works.

Ag NPs were found in mussels' tissues by TEM imaging and significant accumulation of Ag in mussels is observed upon exposure by feed intake suggesting that Ag NPs are significantly accumulated and internalized in mussel's tissues.

A slight accumulation of Zn was detected in mussel's tissues upon exposure by feed intake to ZnO NPs in the bioaccumulation assays. However, this accumulation is reversed in the last time point, which could be due to impairment of mussel correct respiration and subsequent stress response. Internalization of ZnO NPs could not be verified by TEM.

This study reports for the first time the significant adhesion of TiO₂ and ZnO NPs to the exposed mussel's shell, which could have important implications in risk assessment for seafood consumption by humans.

V. Future perspectives

Further investigation should be performed in bioaccumulation of environmentally relevant NPs in animal models, with particular attention to human consumption products, in order to be able to perform a good risk assessment of human intake.

The optimization of biological samples digestion protocols is a must in order to obtain high recovery rates for TiO₂ and ZnO NPs but following safe and profitable procedures. Great efforts are being performed nowadays in this direction, but further developments are expected.

The optimization in the biological specimen preparation for inorganic nanomaterials imaging and chemical analysis by Electron microscopy (SEM and TEM) and EDX should be continued in order to be able to confirm the presence of nanoparticles in the tissue. Contrasting techniques should be encompassed by high resolution techniques that allow the elemental identification in such complex matrix where small conductive NPs must be found in no conductive matrix (biological tissues).

Studies on the interaction of ENMs with organisms in the basis of the food webs will help to understand the mechanisms behind the internalization of the ENMs in higher trophic levels, allowing to better predict risks associated with other particles.

VI. References

- [1] Kaur, I., Kakkar, V., Deol, P., Yadav, M., Singh, M. and Sharma, I. (2014). Issues and concerns in nanotech product development and its commercialization. *Journal of Controlled Release*, 193, pp.51-62.
- [2] Maynard, R. (2012). Nano-technology and nano-toxicology. *Emerging Health Threats Journal*, 5(1), p.17508.
- [3] Akkoyun, M. and Suvaci, E. (2016). Effects of TiO₂, ZnO, and Fe₃O₄ nanofillers on rheological behavior, microstructure, and reaction kinetics of rigid polyurethane foams. *Journal of Applied Polymer Science*, 133(28).
- [4] Cruz, S. and Viana, J. (2015). Structure-Properties Relationships in Thermoplastic Polyurethane Elastomer Nanocomposites: Interactions between Polymer Phases and Nanofillers. *Macromolecular Materials and Engineering*, 300(11), pp.1153-1162.
- [5] Kim, D., Lee, J., Hwang, T., Oh, J., Hong, J., Lee, P., Seferis, J. and Nam, J. (2011). *Nanofillers*. Wiley Encyclopedia of Composites.
- [6] Basto, M., Nicastro, K., Tavares, A., McQuaid, C., Casero, M., Azevedo, F. and Zardi, G. (2019). Plastic ingestion in aquatic birds in Portugal. *Marine Pollution Bulletin*, 138, pp.19-24.
- [7] Machovsky-Capuska, G., Amiot, C., Denuncio, P., Grainger, R. and Raubenheimer, D. (2019). A nutritional perspective on plastic ingestion in wildlife. *Science of The Total Environment*, 656, pp.789-796.
- [8] Plastics Europe; Annual Review 2017-2018
- [9] Basto, M., Nicastro, K., Tavares, A., McQuaid, C., Casero, M., Azevedo, F. and Zardi, G. (2019). Plastic ingestion in aquatic birds in Portugal. *Marine Pollution Bulletin*, 138, pp.19-24.
- [10] Borrelle, S., Rochman, C., Liboiron, M., Bond, A., Lusher, A., Bradshaw, H. and Provencher, J. (2017). Opinion: Why we need an international agreement on marine plastic pollution. *Proceedings of the National Academy of Sciences*, 114(38), pp.9994-9997.
- [11] Singh, A. (2015), Nanoparticle Ecotoxicology. In: A. Singh, ed., *Engineered Nanoparticles*, 1st ed. Elsevier Science Publishing CO INC.
- [12] Bergmann, M., Mützel, S., Primpke, S., Tekman, M., Trachsel, J. and Gerdtts, G. (2019). White and wonderful? Microplastics prevail in snow from the Alps to the Arctic. *Science Advances*, 5(8), pp.1157.
- [13] Miranda, D. and de Carvalho-Souza, G. (2016). Are we eating plastic-ingesting fish? *Marine Pollution Bulletin*, 103(1-2), pp.109-114.
- [14] Davidson, K. and Dudas, S. (2016). Microplastic Ingestion by Wild and Cultured Manila Clams (*Venerupis philippinarum*) from Baynes Sound, British Columbia. *Archives of Environmental Contamination and Toxicology*, 71(2), pp.147-156.
- [15] Stafford, R. and Jones, P. (2019). Viewpoint – Ocean plastic pollution: A convenient but distracting truth? *Marine Policy*, 103, pp.187-191.
- [16] Worm, B. (2015). Silent spring in the ocean. *Proceedings of the National Academy of Sciences*, 112(38), pp.11752-11753.

- [17] Singh, A. (2015), Human and Environmental Risk Characterization of Nanoparticles. In: A. Singh, ed., *Engineered Nanoparticles*, 1st ed. Elsevier Science Publishing CO INC.
- [18] Echa.europa.eu. (2019). Homepage - ECHA. [online] Available at: <https://echa.europa.eu/home> [Accessed 21 Oct. 2019]
- [19] European Commission. 2011a. Commission Recommendation of 18 October 2011 on the definition of nanomaterial. Official J Eur Union L 275:38–40.
- [20] Lützhøft, H., Hartmann, N., Brinch, A., Kjølholt, J. and Baun, A. (2015). Environmental effects of engineered nanomaterials: Estimations of Predicted No-Effect Concentrations (PNECs). Danish Environmental Protection Agency.
- [21] Ullah Khan, S., Saleh, T., Wahab, A., Ullah Khan, M., Khan, D., Ullah Khan, W., Rahim, A., Kamal, S., Ullah Khan, F. and Fahad, S. (2018). Nanosilver: new ageless and versatile biomedical therapeutic scaffold. *International Journal of Nanomedicine*, Volume 13, pp.733-762.
- [22] Durán, N., Silveira, C., Durán, M. and Martinez, D. (2015). Silver nanoparticle protein corona and toxicity: a mini review. *Journal of Nanobiotechnology*, 13(1).
- [23] Zhang, X., Liu, Z., Shen, W. and Gurunathan, S. (2016). Silver Nanoparticles: Synthesis, Characterization, Properties, Applications, and Therapeutic Approaches. *International Journal of Molecular Sciences*, 17(9), p.1534.
- [24] Rajala, J., Vehniäinen, E., Väisänen, A. and Kukkonen, J. (2018). Toxicity of silver nanoparticles to *Lumbriculus variegatus* is a function of dissolved silver and promoted by low sediment pH. *Environmental Toxicology and Chemistry*, 37(7), pp.1889-1897.
- [25] Li, Y. and Chen, T. (2014). Genotoxicity of Silver Nanoparticles. *Handbook of Nanotoxicology, Nanomedicine and Stem Cell Use in Toxicology*, pp.87-98.
- [26] de Lima, R., Seabra, A. and Durán, N. (2012). Silver nanoparticles: a brief review of cytotoxicity and genotoxicity of chemically and biogenically synthesized nanoparticles. *Journal of Applied Toxicology*, 32(11), pp.867-879.
- [27] Mosselhy, D., He, W., Li, D., Meng, Y. and Feng, Q. (2016). Silver nanoparticles: in vivo toxicity in zebrafish embryos and a comparison to silver nitrate. *Journal of Nanoparticle Research*, 18(8).
- [28] Chowdhury, I., Hong, Y., Honda, R. and Walker, S. (2011). Mechanisms of TiO₂ nanoparticle transport in porous media: Role of solution chemistry, nanoparticle concentration, and flowrate. *Journal of Colloid and Interface Science*, 360(2), pp.548-555.
- [29] Bourgeault, A., Cousin, C., Geertsen, V., Cassier-Chauvat, C., Chauvat, F., Durupthy, O., Chanéac, C. and Spalla, O. (2015). The Challenge of Studying TiO₂ Nanoparticle Bioaccumulation at Environmental Concentrations: Crucial Use of a Stable Isotope Tracer. *Environmental Science & Technology*, 49(4), pp.2451-2459.
- [30] Shi, H., Magaye, R., Castranova, V. and Zhao, J. (2013). Titanium dioxide nanoparticles: a review of current toxicological data. *Particle and Fiber Toxicology*, 10(1), p.15.
- [31] Ni, M., Leung, M., Leung, D. and Sumathy, K. (2007). A review and recent developments in photocatalytic water-splitting using TiO₂ for hydrogen production. *Renewable and Sustainable Energy Reviews*, 11(3), pp.401-425.

- [32] Moongraksathum, B. and Chen, Y. (2018). Anatase TiO₂ co-doped with silver and ceria for antibacterial application. *Catalysis Today*, 310, pp.68-74.
- [33] Cupi, D., N. Sørensen, S., M. Skjolding, L. and Baun, A. (2016). Toxicity of Engineered Nanoparticles to Aquatic Invertebrates. In: Xing, B., Vecitis, C., D., and Senesi, N., ed., *Engineered Nanoparticles and the Environment: Biophysicochemical Processes and Toxicity*, 1st ed. John Wiley & Sons, Inc., p.375.].
- [34] Barmo, C., Ciacci, C., Canonico, B., Fabbri, R., Cortese, K., Balbi, T., Marcomini, A., Pojana, G., Gallo, G. and Canesi, L. (2013). In vivo effects of n-TiO₂ on digestive gland and immune function of the marine bivalve *Mytilus galloprovincialis*. *Aquatic Toxicology*, 132-133, pp.9-18.
- [35] Balbi, T., Smerilli, A., Fabbri, R., Ciacci, C., Montagna, M., Grasselli, E., Brunelli, A., Pojana, G., Marcomini, A., Gallo, G. and Canesi, L. (2014). Co-exposure to n-TiO₂ and Cd₂₊ results in interactive effects on biomarker responses but not in increased toxicity in the marine bivalve *M. galloprovincialis*. *Science of The Total Environment*, 493, pp.355-364.
- [36] Corsi, I., Cherr, G., Lenihan, H., Labille, J., Hasselov, M., Canesi, L., Dondero, F., Frenzilli, G., Hristozov, D., Pundes, V., Della Torre, C., Pinsino, A., Libralato, G., Marcomini, A., Sabbioni, E. and Matranga, V. (2014). Common Strategies and Technologies for the Ecosafety Assessment and Design of Nanomaterials Entering the Marine Environment. *ACS Nano*, 8(10), pp.9694-9709.
- [37] Canesi, L., Ciacci, C. and Balbi, T. (2017). Invertebrate Models for Investigating the Impact of Nanomaterials on Innate Immunity: The Example of the Marine Mussel *Mytilus* spp. *Current Bionanotechnology*, 2(2), pp.77-83.
- [38] Auguste, M., Lasa, A., Pallavicini, A., Gualdi, S., Vezzulli, L. and Canesi, L. (2019). Exposure to TiO₂ nanoparticles induces shifts in the microbiota composition of *Mytilus galloprovincialis* hemolymph. *Science of The Total Environment*, 670, pp.129-137.
- [39] Ec.europa.eu. (2019). [online] Available at: <https://ec.europa.eu/transparency/regexpert/index.cfm?do=groupDetail.groupMeetingDoc&docid=34559> [Accessed 21 Oct. 2019].
- [40] Smeraldi, J., Ganesh, R., Hosseini, T., Khatib, L., Olson, B. and Rosso, D. (2017). Fate and Toxicity of Zinc Oxide Nanomaterial in Municipal Wastewaters. *Water Environment Research*, 89(9), pp.880-889.
- [41] Choi, S., Baek, M., Chung, H., Yu, J., Lee, J., Kim, T., Oh, J., Lee, W., Paek, S., Lee, J., Jeong, J. and Choy, J. (2012). Pharmacokinetics, tissue distribution, and excretion of zinc oxide nanoparticles. *International Journal of Nanomedicine*, p.3081.
- [42] Li, L., Zhou, D., Peijnenburg, W., van Gestel, C., Jin, S., Wang, Y. and Wang, P. (2011). Toxicity of zinc oxide nanoparticles in the earthworm, *Eisenia fetida* and subcellular fractionation of Zn. *Environment International*, 37(6), pp.1098-1104.
- [43] Li, J., Schiavo, S., Xiangli, D., Rametta, G., Miglietta, M., Oliviero, M., Changwen, W. and Manzo, S. (2018). Early ecotoxic effects of ZnO nanoparticle chronic exposure in *Mytilus galloprovincialis* revealed by transcription of apoptosis and antioxidant-related genes. *Ecotoxicology*, 27(3), pp.369-384.
- [44] Sudoenanodesk.net. (2019). [online] Available at: http://sudoenanodesk.net/public/docs/deliverables/DA1a.%20Report%20on%20the%20applications%20of%20ENMs%20in%20the%20plastic%20sector_v4.pdf [Accessed 21 Oct. 2019].
- [45] Nowack, B. and Bucheli, T. (2007). Occurrence, behavior and effects of nanoparticles in the environment. *Environmental Pollution*, 150(1), pp.5-22.

- [46] Seed, R. and Suchanek, T. (1993). The mussel, *Mytilus*: Ecology, Physiology, genetics and culture. *Comparative Biochemistry and Physiology Part A: Physiology*, 105(2), p.381.
- [47] Speciale, A., Zena, R., Calabrò, C., Bertuccio, C., Aragona, M., Saija, A., Trombetta, D., Cimino, F. and Lo Cascio, P. (2018). Experimental exposure of blue mussels (*Mytilus galloprovincialis*) to high levels of benzo[a]pyrene and possible implications for human health. *Ecotoxicology and Environmental Safety*, 150, pp.96-103.
- [48] Gosling, E. (2003). *Bivalve Mollusks: Biology, Ecology and Culture*. 1st ed. Fishing News Books.
- [49] Uslu, F. and Pekkan, K. (2016). *Mytilus galloprovincialis* as a smart micro-pump. *Biology Open*, 5(10), pp.1493-1499.
- [50] Prego-Faraldo, M., Valdiguésias, V., Laffon, B., Mendez, J. and Eirin-Lopez, J. (2016). Early Genotoxic and Cytotoxic Effects of the Toxic Dinoflagellate *Prorocentrum lima* in the Mussel *Mytilus galloprovincialis*. *Toxins*, 8(6), p.159.
- [51] Canesi, L., Ciacci, C., Vallotto, D., Gallo, G., Marcomini, A. and Pojana, G. (2010). In vitro effects of suspensions of selected nanoparticles (C60 fullerene, TiO₂, SiO₂) on *Mytilus* hemocytes. *Aquatic Toxicology*, 96(2), pp.151-158.
- [52] Scientific, Technical and Economic Committee for Fisheries (STECF) – The economic performance of the EU aquaculture sector (STECF 14-18). (2014). *Publications Office of the European Union*, Luxembourg.
- [53] Parisi, M., Mauro, M., Sarà, G. and Cammarata, M. (2017). Temperature increases, hypoxia, and changes in food availability affect immunological biomarkers in the marine mussel *Mytilus galloprovincialis*. *Journal of Comparative Physiology B*, 187(8), pp.1117-1126.
- [54] Goldberg, E. (1975). The mussel watch – A first step in global marine monitoring. *Marine Pollution Bulletin*, 6(7), p.111-113.
- [55] Sericano, J., Wade, T., Jackson, T., Brooks, J., Tripp, B., Farrington, J., Mee, L., Readmann, J., Villeneuve, J. and Goldberg, E. (1995). Trace organic contamination in the Americas: An overview of the US National Status & Trends and the International ‘Mussel Watch’ programmes. *Marine Pollution Bulletin*, 31(4-12), pp.214-225.
- [56] Casas, S., Gonzalez, J., Andral, B. and Cossa, D. (2007). Relation Between Metal Concentration in Water and Metal Content of Marine Mussels: Impact of Physiology. *Environmental Toxicology and Chemistry*, (2008), p.1.
- [57] Auguste, M., Ciacci, C., Balbi, T., Brunelli, A., Caratto, V., Marcomini, A., Cuppini, R. and Canesi, L. (2018). Effects of nanosilver on *Mytilus galloprovincialis* hemocytes and early embryo development. *Aquatic Toxicology*, 203, pp.107-116.
- [58] Torres-Duarte, C., Hutton, S., Vines, C., Moore, J. and Cherr, G. (2018). Effects of soluble copper and copper oxide nanoparticle exposure on the immune system of mussels, *Mytilus galloprovincialis*. *Environmental Toxicology*, 34(3), pp.294-302.
- [59] Brandts, I., Teles, M., Gonçalves, A., Barreto, A., Franco-Martinez, L., Tvarijonaviciute, A., Martins, M., Soares, A., Tort, L. and Oliveira, M. (2018). Effects of nanoplastics on *Mytilus galloprovincialis* after individual and combined exposure with carbamazepine. *Science of The Total Environment*, 643, pp.775-784.

- [60] Pittura, L., Avio, C., Giuliani, M., d'Errico, G., Keiter, S., Cormier, B., Gorbi, S. and Regoli, F. (2018). Microplastics as Vehicles of Environmental PAHs to Marine Organisms: Combined Chemical and Physical Hazards to the Mediterranean Mussels, *Mytilus galloprovincialis*. *Frontiers in Marine Science*, 5.
- [61] Mezzelani, M., Gorbi, S., Fattorini, D., d'Errico, G., Consolandi, G., Milan, M., Bargelloni, L. and Regoli, F. (2018). Long-term exposure of *Mytilus galloprovincialis* to diclofenac, Ibuprofen and Ketoprofen: Insights into bioavailability, biomarkers and transcriptomic changes. *Chemosphere*, 198, pp.238-248.
- [62] Stetefeld, J., McKenna, S. and Patel, T. (2016). Dynamic light scattering: a practical guide and applications in biomedical sciences. *Biophysical Reviews*, 8(4), pp.409-427.
- [63] Arzenšek, D. (2010). *Dynamic light scattering and application to proteins in solutions*. University of Ljubljana.
- [64] Vogel, R., Pal, A., Jambhrunkar, S., Patel, P., Thakur, S., Reátegui, E., Parekh, H., Saá, P., Stassinopoulos, A. and Broom, M. (2017). High-Resolution Single Particle Zeta Potential Characterization of Biological Nanoparticles using Tunable Resistive Pulse Sensing. *Scientific Reports*, 7(1).
- [65] Tatro, M. and Amarasiriwardena, D. (2016). Optical Emission Inductively Coupled Plasma in Environmental Analysis. *Encyclopedia of Analytical Chemistry*, pp.1-13.
- [66] Olesik, J. (1991). Elemental analysis using ICP-OES and ICP-MS. *Analytical Chemistry*, 63(1), pp.12A-21A.
- [67] Jiménez-Lamana, J., Laborda, F., Bolea, E., Abad-Álvarez, I., Castillo, J., Bianga, J., He, M., Bierla, K., Mounicou, S., Ouerdane, L., Gaillet, S., Rouanet, J. and Szpunar, J. (2014). An insight into silver nanoparticles bioavailability in rats. *Metallomics*, 6(12), pp.2242-2249.
- [68] Loeschner, K., Brabrand, M., Sloth, J. and Larsen, E. (2013). Use of alkaline or enzymatic sample pretreatment prior to characterization of gold nanoparticles in animal tissue by single-particle ICPMS. *Analytical and Bioanalytical Chemistry*, 406(16), pp.3845-3851.
- [69] Altundag, H. and Tuzen, M. (2011). Comparison of dry, wet and microwave digestion methods for the multi element determination in some dried fruit samples by ICP-OES. *Food and Chemical Toxicology*, 49(11), pp.2800-2807.
- [70] Marguí, E., Queralt, I., Carvalho, M. and Hidalgo, M. (2005). Comparison of EDXRF and ICP-OES after microwave digestion for element determination in plant specimens from an abandoned mining area. *Analytica Chimica Acta*, 549(1-2), pp.197-204.
- [71] Loeschner, K., Navratilova, J., Købler, C., Mølhav, K., Wagner, S., von der Kammer, F. and Larsen, E. (2013). Detection and characterization of silver nanoparticles in chicken meat by asymmetric flow field flow fractionation with detection by conventional or single particle ICP-MS. *Analytical and Bioanalytical Chemistry*, 405(25), pp.8185-8195.
- [72] Bolea, E., Jiménez-Lamana, J., Laborda, F., Abad-Álvarez, I., Bladé, C., Arola, L. and Castillo, J. (2014). Detection and characterization of silver nanoparticles and dissolved species of silver in culture medium and cells by AsFIFFF-UV-Vis-ICPMS: application to nanotoxicity tests. *The Analyst*, 139(5), pp.914-922.
- [73] Gray, E., Coleman, J., Bednar, A., Kennedy, A., Ranville, J. and Higgins, C. (2013). Extraction and Analysis of Silver and Gold Nanoparticles from Biological Tissues Using Single Particle Inductively Coupled Plasma Mass Spectrometry. *Environmental Science & Technology*, 47(24), pp.14315-14323.

- [74] Loeschner, K., Brabrand, M., Sloth, J. and Larsen, E. (2013). Use of alkaline or enzymatic sample pretreatment prior to characterization of gold nanoparticles in animal tissue by single-particle ICP-MS. *Analytical and Bioanalytical Chemistry*, 406(16), pp.3845-3851.
- [75] Tendeloo, G., Van Dyck, D. and Pennycook, S. (2012). *Handbook of nanoscopy*. Weinheim: Wiley-VCH Verlag GmbH & Co KGaA, pp.309, 345.
- [76] Luft, J. (1961). Improvements in epoxy resin embedding methods. *The Journal of Cell Biology*, 9(2), pp.409-414.
- [77] Padua, G. and Wang, Q. (2012). *Nanotechnology research methods for foods and bioproducts*. Ames, Iowa: Wiley-Blackwell, pp.103,111.
- [78] Leng, Y. (2013). *Materials characterization*. Weinheim: J. Wiley, p.121.
- [79] Mueller, N. and Nowack, B. (2008). Exposure Modeling of Engineered Nanoparticles in the Environment. *Environmental Science & Technology*, 42(12), pp.4447-4453.
- [80] Echa.europa.eu. (2019). [online] Available at: <https://echa.europa.eu/documents/10162/596b1f42-8bfe-48f8-86f4-cd98fe6b7041> [Accessed 30 Nov. 2019].
- [81] Gomes, T., Pereira, C., Cardoso, C., Sousa, V., Teixeira, M., Pinheiro, J. and Bebianno, M. (2014). Effects of silver nanoparticles exposure in the mussel *Mytilus galloprovincialis*. *Marine Environmental Research*, 101, pp.208-214.
- [82] Kalle, K. (1971) Salinity: general introduction. In: *Marine Ecology* (ed. O. Kinne), pp.683–88. Wiley-Interscience, New York.
- [83] Bossert, D., Urban, D., Maceroni, M., Ackermann-Hirschi, L., Haeni, L., Yajan, P., Spuch-Calvar, M., Rothen-Rutishauser, B., Rodriguez-Lorenzo, L., Petri-Fink, A. and Schwab, F. (2019). A hydrofluoric acid-free method to dissolve and quantify silica nanoparticles in aqueous and solid matrices. *Scientific Reports*, 9(1).
- [84] Earing, M., Jackson, D., Ash, A. and Aoki, K. (1956). Nitric Acid Oxidation of Polyethylene Glycols and their Monomethyl Ethers. *Industrial & Engineering Chemistry*, 48(9), pp.1467-1468.
- [85] Dumont, E., Johnson, A., Keller, V. and Williams, R. (2015). Nano silver and nano zinc-oxide in surface waters – Exposure estimation for Europe at high spatial and temporal resolution. *Environmental Pollution*, 196, pp.341-349.
- [86] Guascito, M., Filippo, E., Malitesta, C., Manno, D., Serra, A. and Turco, A. (2008). A new amperometric nanostructured sensor for the analytical determination of hydrogen peroxide. *Biosensors and Bioelectronics*, 24(4), pp.1057-1063.
- [87] Baveye, P. and Laba, M. (2008). Aggregation and Toxicology of Titanium Dioxide Nanoparticles. *Environmental Health Perspectives*, 116(4).
- [88] Hanna, S., Miller, R., Muller, E., Nisbet, R. and Lenihan, H. (2013). Impact of Engineered Zinc Oxide Nanoparticles on the Individual Performance of *Mytilus galloprovincialis*. *PLOS ONE*, 8(4), p.e61800.